UNITED NATIONS UNIVERSITY
GEOTHERMAL TRAINING PROGRAMME
Orkustofnun, Grensasvegur 9,
IS-108 Reykjavik, Iceland

Report 2011
Number 22

INITIAL CONDITIONS OF WELLS OW-906A, OW-908, OW-910A AND OW-914 AND A SIMPLE NATURAL STATE MODEL OF OLKARIA DOMES GEOTHERMAL FIELD, KENYA

Urbanus Kioko Mbithi
Kenya Electricity Generating Company - KenGen
P.O. Box 785-20117
Naivasha
KENYA
umbithi@kengen.co.ke, urbanuskioko@yahoo.co.uk

ABSTRACT

The Greater Olkaria geothermal area is divided into seven sectors. Currently, three sectors are generating about 202 MWe and production drilling for the Domes has been completed. Plans are now at an advanced stage to set up a 140 MWe power plant in the Olkaria Domes field. Systematic analysis of downhole temperature and pressure profiles, injection, fall-off and discharge tests has given the basis for a conceptual reservoir model for the Domes. The reservoir is two phase with the temperature following the boiling point curve; logging revealed temperatures of over 300°C in most of the wells at a depth of about 2000 m. The conceptual model shows that the Domes field has an upflow zone near wells OW-909, OW-910, OW-915 and OW-915. Fluid flow appears to be generally from northeast to southwest and well OW-902 seems to have been drilled in an outflow zone. Well test analysis indicate transmissivities in the range 1.5-4.6 × 10^{-8} m^3/Pa.s and effective permeabilities of 3.1-5.9 mD in the reservoir, with negative skin being observed in most of the wells. Injectivities of the wells range from 3.5 to 3.6 (L/s)/bar.

1. INTRODUCTION

The eastern arm of the East African Rift transects Kenya in a N-S direction. The area has a number of quaternary volcanoes on the floor of the Rift Valley where most of the East African lakes are found. Many of these lakes are salty but a few of them have fresh water which acts as a recharge to geothermal systems (Lagat, 2004). The major exemption is Lake Victoria that lies in the depression between the western and eastern parts of the Rift Valley. Quaternary volcanism has led to geothermal manifestations such as fumaroles, steam jets, hot springs, geysers, hot mud pools and hydrothermal rock alterations in many parts of the Kenyan Rift Valley.

There are, however, exceptions with a few geothermal resources occurring outside the Kenyan Rift Valley. These off-axis Quaternary volcanoes, such as Homabay, Jombo Hills, Chogoria and Maji Moto, all exhibit low-enthalpy characteristics. Fourteen geothermal prospects have been identified within the Kenyan Rift Valley starting from Barrier in the north to Lake Magadi in the south with a potential of over 3000 MWe (Figure 1). Areas with geothermal systems are also associated with high local fluxes and a high temperature gradient of about 120°C/km.

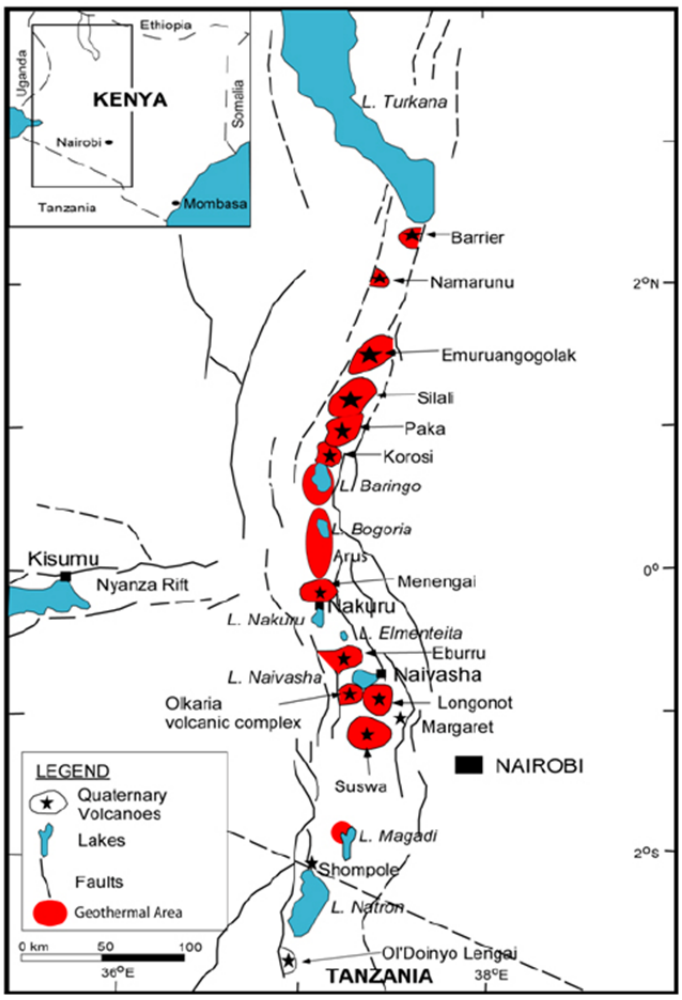

FIGURE 1: Location map of geothermal prospects in the Kenyan Rift Valley (Were, 2007)

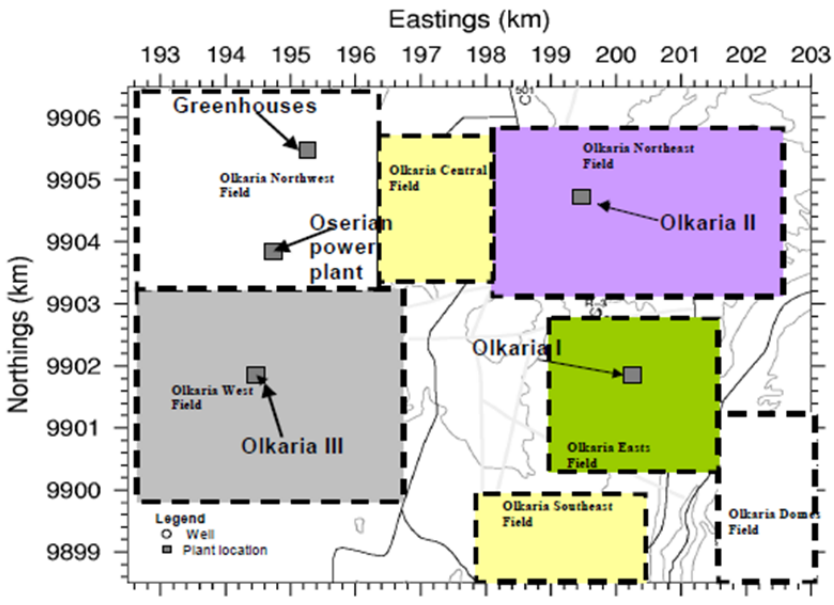

FIGURE 2: Geothermal sectors in the Greater Olkaria geothermal area

The Greater Olkaria geothermal field is in the southern part of the Kenyan Rift. It is located south of Lake Naivasha, approximately 120 km northwest of Nairobi city. The field is divided into seven fields for the sake of development. The different parts are: Olkaria Central, Olkaria East, Olkaria Northeast, Olkaria Northwest, Olkaria Southeast, Olkaria Southwest and Olkaria Domes (Figure 2). Exploitation in the field started in 1981 when Olkaria 1 power plant, with a 15 MWe turbine, was commissioned. The power plant is in Olkaria East, a part of the Greater Olkaria field. The second and third turbines, each 15 MWe, were commissioned in 1982 and 1985, respectively. This pioneer power plant is still in place today, producing 45 MWe although it has completed its designed plant life. Currently the steam available in Olkaria East field is more than what is required to generate 45 MWe and production drilling is underway to increase generation by adding two 70 MWe units (Olkaria IV and V).

Additional power plants have been installed in Olkaria recently. These include Olkaria II, which is in Olkaria Northeast, commissioned in 2003. The plant has been generating 70 MWe but an additional 35 MWe turbine was commissioned in May 2010, increasing the capacity to 105 MWe. Olkaria Southwest field hosts Olkaria III, an Independent Power Producer (IPP) binary power plant. It generates 48 MWe; the first 12 MWe unit was commissioned in 2000 and the second 36 MWe was established in 2009. Another binary plant at Olkaria Northwest (Oserian) was commissioned in 2004, with a capacity of 2 MWe.

Exploration was done in Eburru between 1988 and 1990. Six wells were drilled and plans are underway to put up a 2.5 MWe power plant.

Exploration drilling was also undertaken in other sectors of Olkaria, the most recent being in the Olkaria Domes field, located south of the Olkaria East field. Surface exploration in Olkaria Domes field was completed in 1993 and drilling of three exploration wells was carried out in 1998-1999. Drilling of 6 appraisal wells started in 2007 and the results from the drilled wells updated the conceptual model which led to the siting and drilling of the production wells which have now been completed. Plans are at an advanced stage to put up a 140 MWe power plant (Olkaria IV), implementing two 70 MWe units, and is anticipated to be commissioned in the years 2012 and 2013, respectively.

In this report, a reservoir conceptual model and assessment study is put forward. The report covers downhole temperature and pressure in four wells in the Domes field and a few surrounding wells.

2. AN OVERVIEW OF OLKARIA DOMES GEOTHERMAL FIELD

2.1 Geological setting

The Greater Olkaria volcanic complex is characterised by numerous volcanic centres of quaternary age and is the only area within the Kenyan Rift with the occurrence of comedite on the surface (Lagat, 2004). The structures in the Olkaria volcanic complex include: The Ol´Njorowa gorge, the ENE-WSW Olkaria fault and N-S, NNE-SSW, NW-SE and WNW-ESE trending faults (Figure 3). The faults are more prominent in the East, Northeast and West Olkaria fields but are scarce in the Olkaria Domes area, possibly due to a thick pyroclastic cover. The NW-SE and WNW-ESE faults are thought to be the oldest and are associated with the development of the rift. The most prominent of these faults is the Gorge Farm fault, which bounds the geothermal fields in the northeast part and extends to the Olkaria Domes area (Lagat, 1995).

The geothermal reservoir is considered to be bound by arcuate faults forming a ring or a caldera structure. A magmatic heat source might be represented by intrusions at deep levels inside the ring structure.

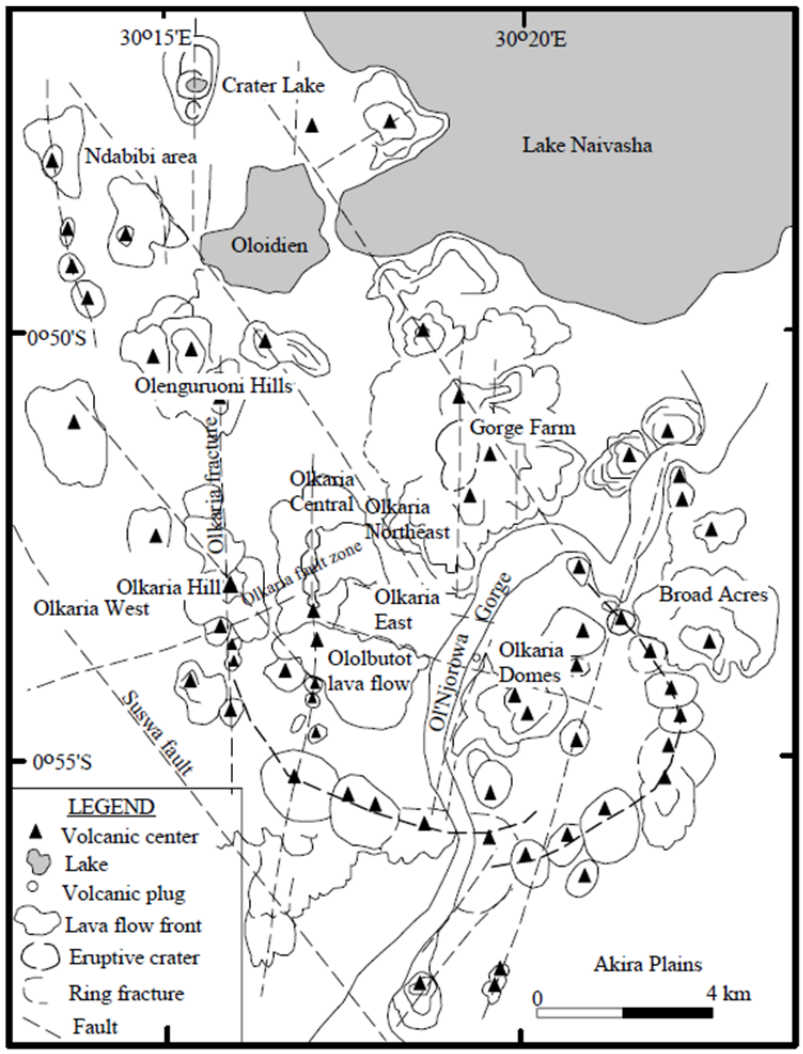

FIGURE 3: Volcanic-tectonic map of the Greater Olkaria geothermal complex (Lagat, 2004)

2.2 Geophysical setting

A gravity survey of the shallow crust beneath Olkaria indicates a volcanic zone of three layers that appears down-faulted in the Olkaria West area and shows low density (Mariita, 2010). The gravity survey further revealed the presence of dense dike material along the Ololbutot fault zone. A Bouguer anomaly map using a density of 2.5 g/cm^3 (Figure 4) shows the following features:

a) A northwest trending axial gravity high corresponding to the regional geological structure in the central rift segment.
b) A low-gravity anomaly that occurs in the west towards the Mau escarpment. Another gravity low occurs in the eastern Olkaria Domes area and extends to Longonot.

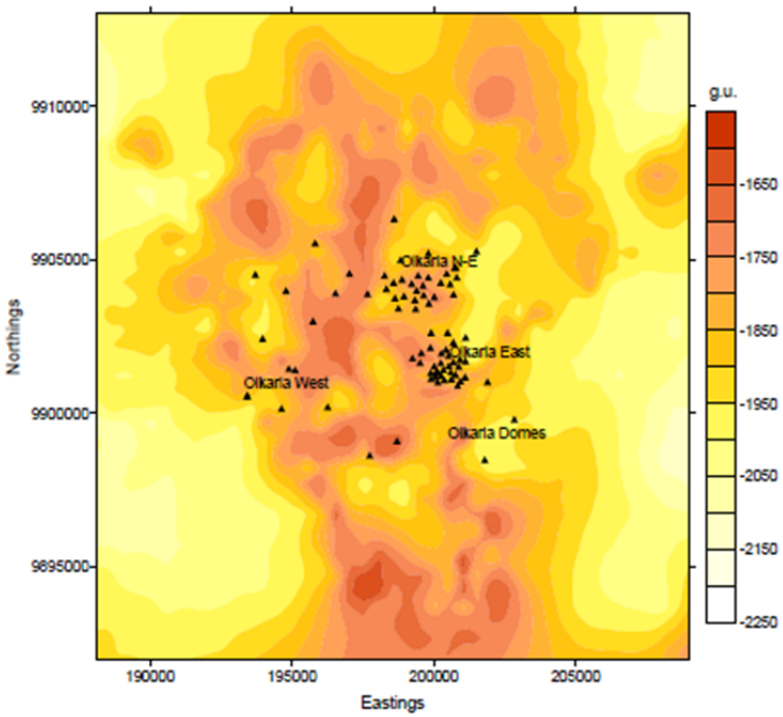

FIGURE 4: Gravity distribution at the Olkaria geothermal field (Omenda, 1998)

2.3 Geochemical setting

Figure 5 shows three Olkaria Domes wells (OW-904B, OW-903B and OW-909) plotting in the region of high HCO_3 peripheral waters and low chloride. This illustrates that the geothermal fluids in the Olkaria Domes reservoir are bicarbonate waters and correspond to peripheral waters (Giggenbach, 1991). The Olkaria Domes field seems to plot similar to those of Olkaria West and Olkaria Central fields (Malimo, 2009).

From the relative abundance of chloride, sulphate and bicarbonate in the Olkaria wells, these waters would be classified as sodium-chloride and sodium-bicarbonate, or mixtures thereof (Figure 5). Wells in the Olkaria East production field and in the Olkaria Northeast discharge sodium-chloride type water, classified as more mature according to the scheme of Giggenbach (1991).

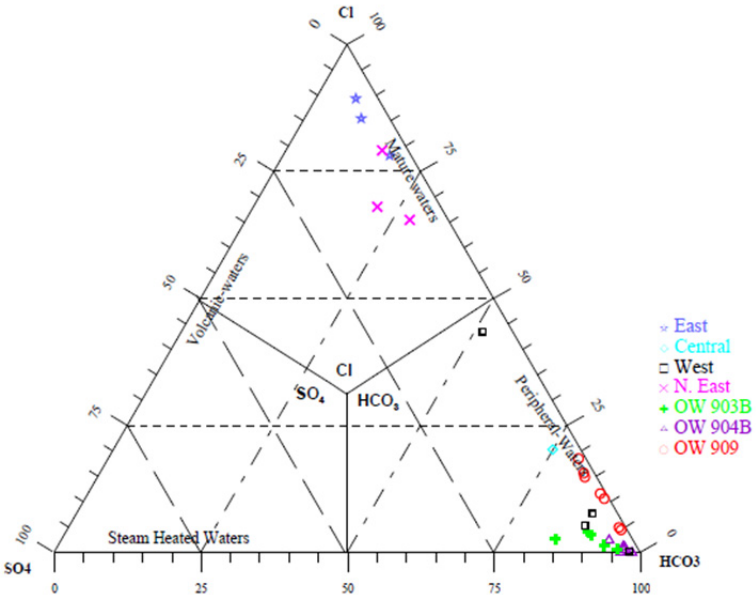

FIGURE 5: Comparative plot of relative Cl-SO_4 - HCO_3 contents from the discharges of wells in the Olkaria field (Malimo, 2009)

3. FORMATION TEMPERATURE AND INITIAL PRESSURE

3.1 General information

Temperature is one of the most important parameters needed for geothermal reservoir analysis. Information obtained from temperature logs can be useful for heat flow estimation, the location of aquifers, and temperature distribution in geothermal reservoirs, as well as reservoir assessment and efficient resource exploitation management. The initial reservoir pressure is also very important. It delineates possible upflow zones of the reservoir as a pressure high or low. It also provides an important reference for analysing production data, including completion tests for estimating reservoir permeability. Repeated pressure logs during warm-up may also show the depth of the major feed zone of the respective well (pivot point analysis).

The cross-correlation of downhole pressure and temperature, with respect to boiling, is necessary in natural state analysis. Geothermal reservoirs often are characterised by vertical cross-flow of water and steam (heat pipe). In this depth interval, pressure and temperature follow the so-called boiling point with a depth curve (BPD) (Björnsson, 2011). In the following analysis of downhole data, the BPD is used for estimating phase conditions of the Olkaria Domes field reservoir.

In this section, we analyse the logs obtained immediately after drilling, during injection tests and the recovery period. Based on this analysis, a formation temperature and initial pressure profiles are presented for wells OW-908, OW-910A, OW-914 and OW-906A.

Temperatures recorded immediately after drilling are generally lower than the true formation temperature. These low temperatures result because the formation is cooled by the circulating drilling fluid. As soon as circulation stops, the temperature around the wellbore begins to recover. However, due to cooling, it is not possible to measure the formation temperature directly. Even if months or years have passed, boiling or convection may occur in the well, making it impossible to probe the formation.

A computer software program, BERGHITI, was developed at Orkustofnun, (Helgason, 1993). It is used for the estimation of formation temperature during recovery after drilling. It offers two methods of calculation: the Albright and the Horner methods.

The *Albright method* is used for direct determination of bottom-hole formation temperatures during economically acceptable interruptions in drilling operations. It assumes an arbitrary time interval, shorter than the total recovery time, and that the temperature relaxation depends only on the difference between the borehole and the formation temperature. This method is commonly applied to warm-up time series shorter than 24 hours.

The *Horner method* is an analysis based on a straight line relationship between temperature, T and the logarithm of relative time, τ, where τ is given by:

$$\tau = \frac{\Delta t}{\Delta t + t_o} \tag{1}$$

where Δt = The time passed since circulation stopped;
t_o = The circulation time.

It is evident that $\lim (\ln \tau) = 0$ for $\Delta t \rightarrow \infty$. Using this and the fact that the system must have stabilised after infinite time, a plot of downhole temperature as a function of $\ln \tau$ yields a straight line. Extrapolating the line to $\ln \tau = 0$ we are able to estimate the formation temperature. Note that this method is only valid for wells with no internal flow, thus it applies only to conductive warm-up.

The Horner method was applied systematically to the downhole temperature data collected so far from Olkaria Domes geothermal field. The calculated formation temperatures were substituted into the PREDYP program to estimate reservoir pressure. The program calculates pressure in a static water column, if the temperature of the column is known (Arason and Björnsson, 1994). Also required for the calculations is either the water level or the well-head pressure. Water level was adjusted in the calculations until the calculated profile matched the pivot point pressure.

3.2 Temperature and pressure profiles

It is of interest to find the undisturbed temperature and pressure conditions in the Olkaria Domes wells. The temperature and pressure recovery trend helps in determining the location of feed zones as well as in developing the initial temperature and pressure. In this section, all available temperature and pressure data of the four Olkaria Domes wells are plotted and analysed in terms of formation temperature and initial pressure. Computer program BOILCURVE (Arason et al., 2003) was used to estimate the boiling conditions. Note that the Horner method is used extensively for all the wells. Table 1 shows the wells' total drilled depths, orientation and the casing depths.

TABLE 1: Olkaria Domes well properties

Well no.	Orientation	Total drilled depth (m)	Casing depth (m)
OW-906A	Deviated	2804	1259
OW-908	Vertical	2988	1201
OW-910A	Deviated	2882	956
OW-914	Vertical	3000	952

Well OW- 906A: The temperature and pressure profiles (Figure 6) show existence of a shallow feed

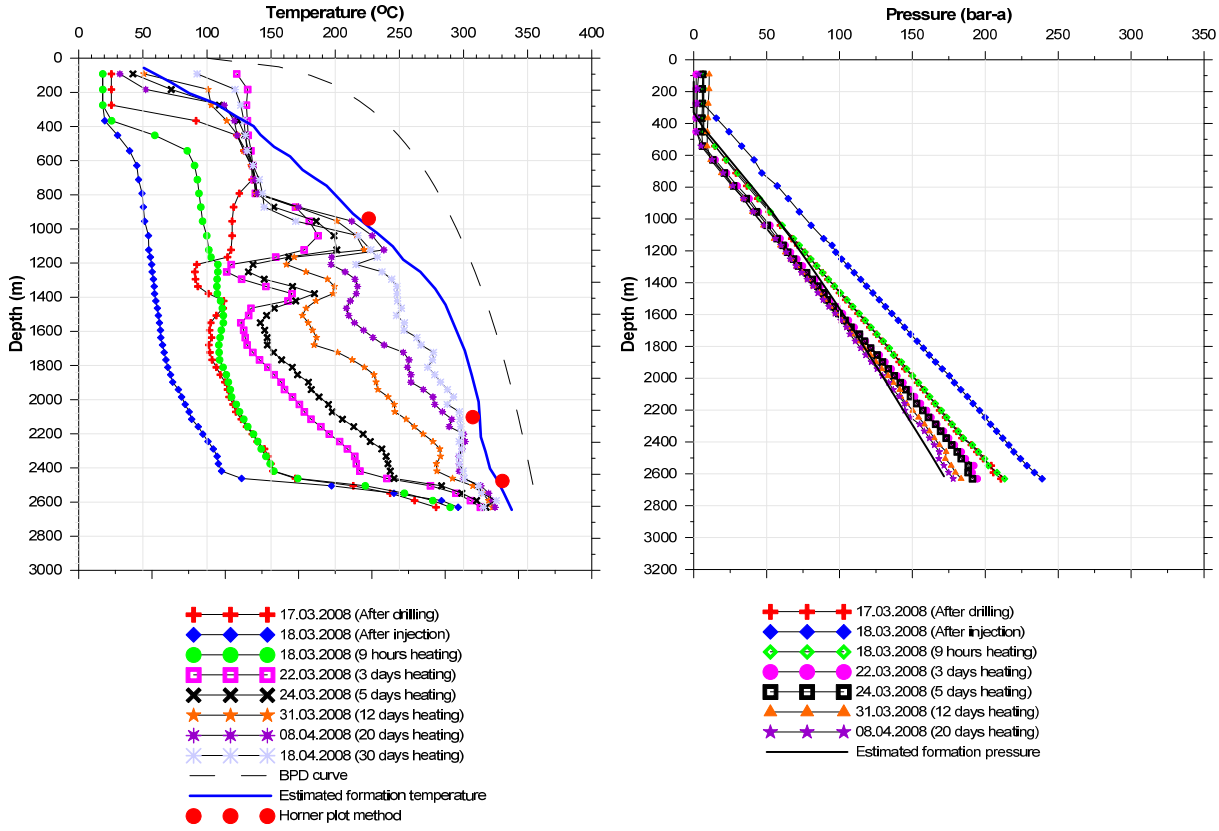

FIGURE 6: OW-906A temperature profiles (left) and pressure profiles (right)

zone below the production casing, producing saturated water at about 250°C. Major feed zones are observed around 1500 and 1800 m depths. Another feed zone could also be observed at around 2400 m depth. The pressure profiles do not show a clear pivot point in this well.

Well OW-908: All downhole temperature profiles are shown in Figure 7. The temperature profiles show a high temperature gradient in the upper and lower parts of the well which could suggest conductive heat transfer through the formation and consequently lower permeability in the surrounding formations. From 1250 to about 1900 m depths, there is a much lower temperature gradient which may be attributed to a convective system along the feed zones. The major feed zone for this well is observed at around 1600 to 1900 m depth.

Well OW-910A: The temperature logs (Figure 8) taken immediately after drilling and over 4 days of heating showed sudden inversions in the temperature profiles at about 1050 m depth. This could be due to cold drilling fluid in the formation which also indicates a permeable zone at this location. The latest profile (29 days of heating) was almost isothermal for depths between 1200 and 1800 m. The feed zones are located at 1050, 1800 m and at the well´s bottom. The temperature inversion observed at the well's bottom might be due to cooling effects of the drilling fluids. The pressure profiles (Figure 8) show the pivot point at around 1800 m and, therefore, the feed zone at this depth dominates the well.

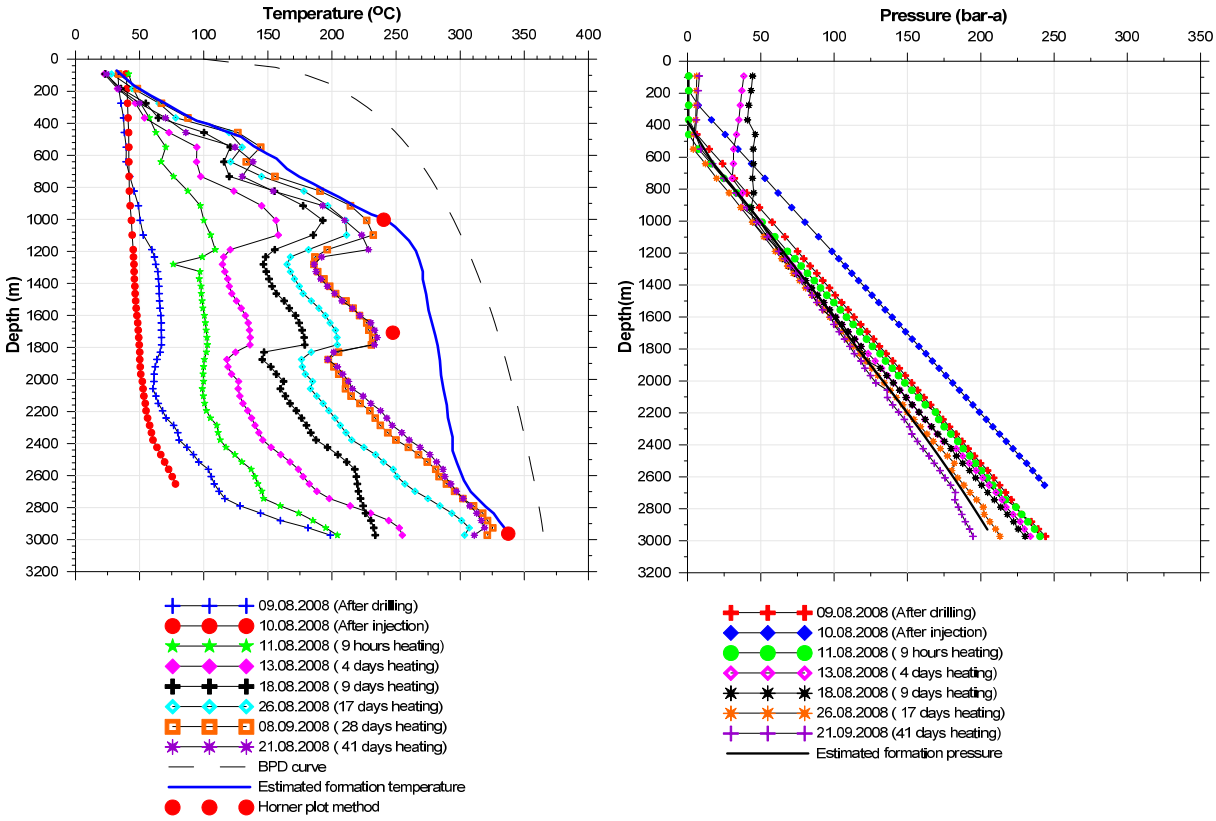

FIGURE 7: OW-908 temperature profiles (left) and pressure profiles (right)

Well OW-914: The shallow feed zone in this well is located at around 1000 m depth, immediately below the production casing depth (Figure 9). The change in the temperature gradient (kicks) observed in all the temperature profiles shows that the other feed zones are located at 1600 and 2200 depths. The measured and initial pressure profiles (Figure 9) show that the pivot point is around 2200 m depth; therefore, the major feed zone is located at this depth.

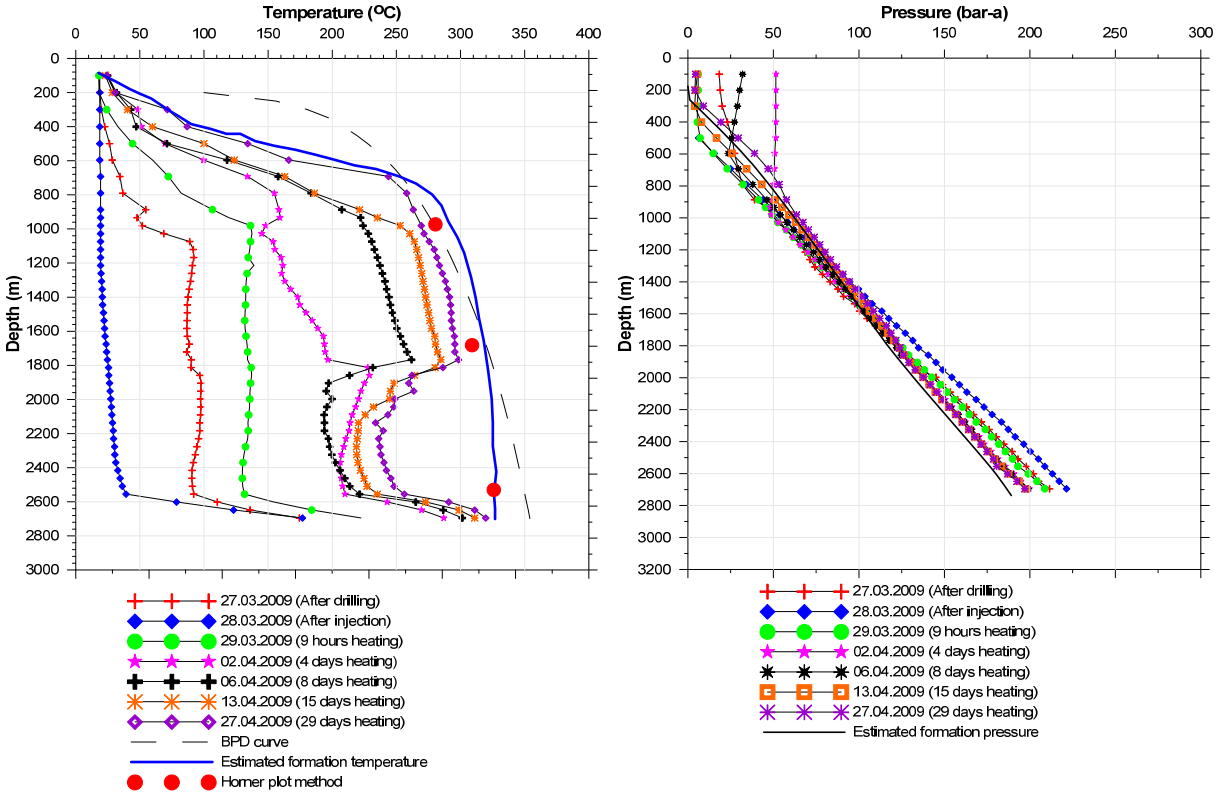

FIGURE 8: OW-910A temperature profiles (left) and pressure profiles (right)

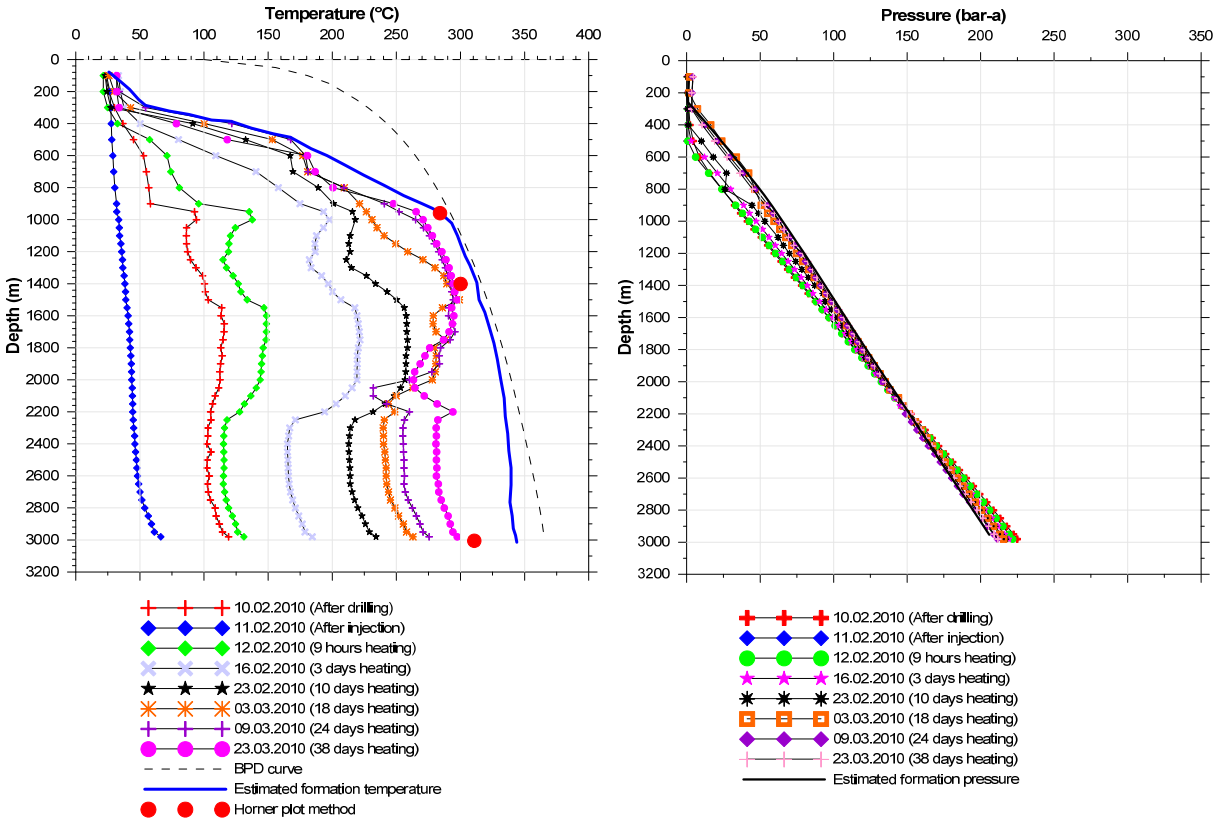

FIGURE 9: OW-914 temperature profiles (left) and pressure profiles (right)

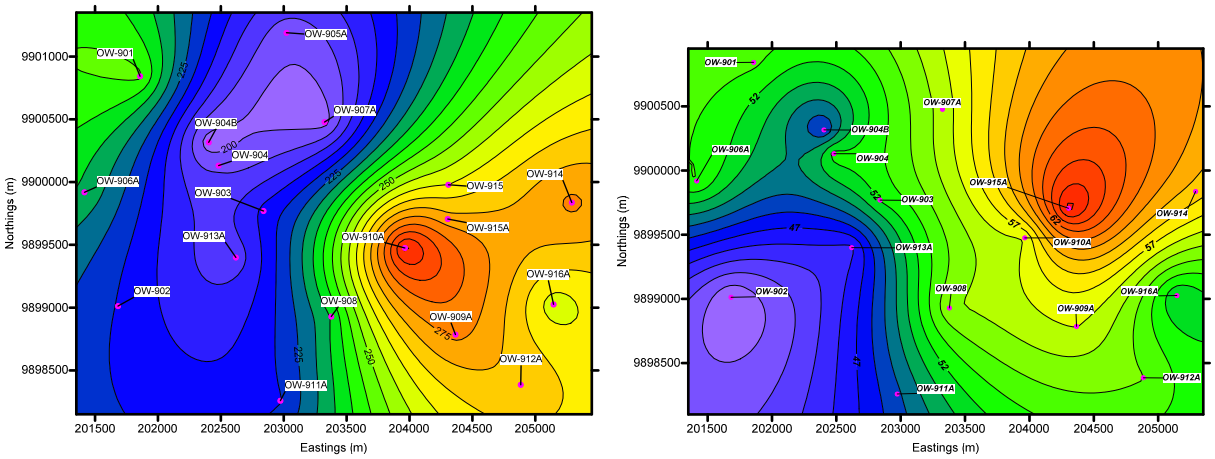

FIGURE 10: Temperature distribution (°C) (left) and pressure (bar-a) (right), at 1000 m a.s.l.

3.3 Temperature and pressure model

In order to define the conceptual reservoir model of the Olkaria Domes geothermal field, three temperature and pressure plane-sections for the whole area were plotted at different elevations. In this project, 1000 m a.s.l., sea level and 600 m b.s.l. (below sea level). were considered. It should be noted that the contours in both horizontal and vertical cross-sections were plotted using estimated formation data (temperature in °C and pressure in bar-a) to represent reservoir conditions. Figures 10, 11 and 12 show temperature and pressure distributions at 1000 m a.s.l., sea level and 600 m b.s.l. The hottest

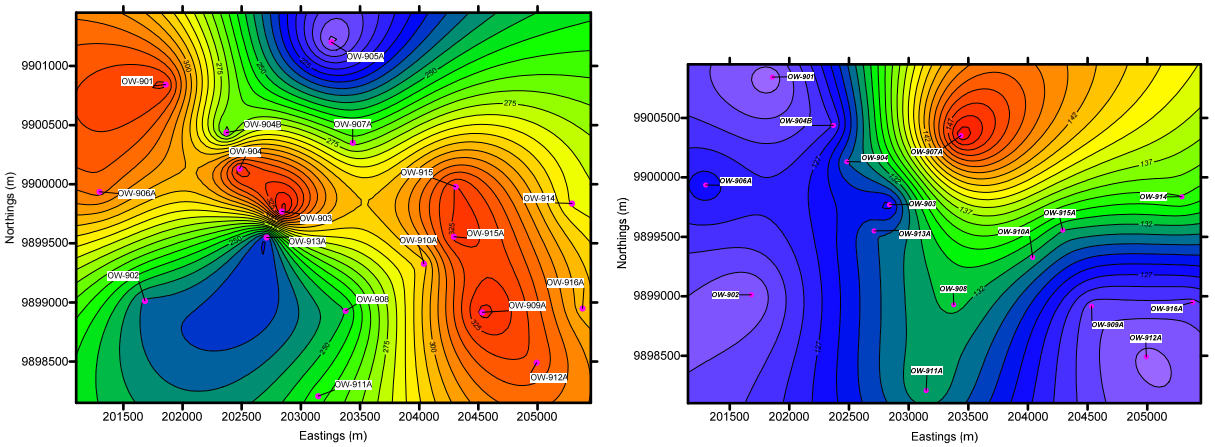

FIGURE 11: Temperature distribution (°C) (left) and pressure (bar-a) (right), at sea level

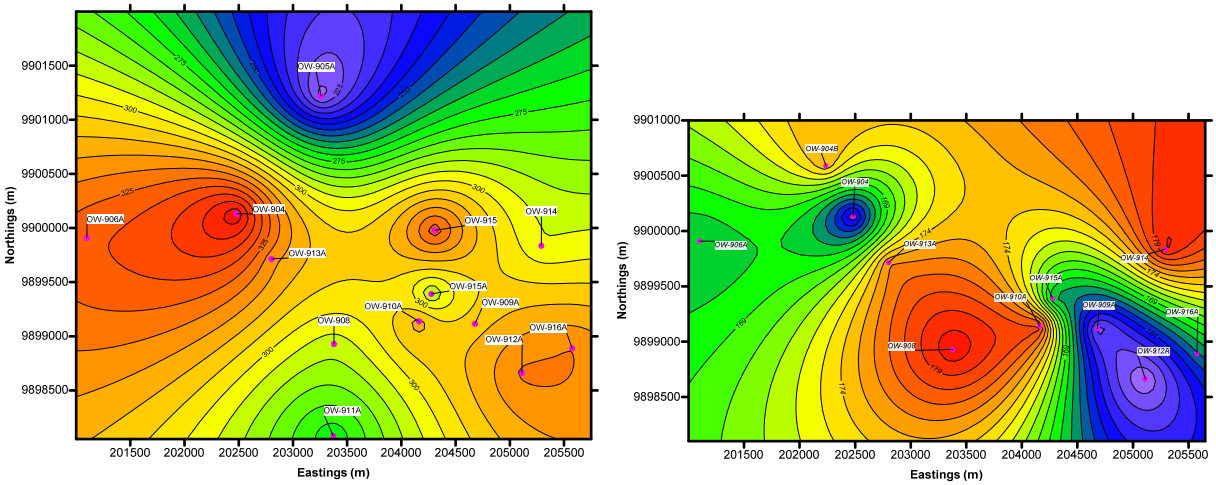

FIGURE 12: Temperature distribution (°C) (left) and pressure (bar-a) (right), at 600 m b.s.l.

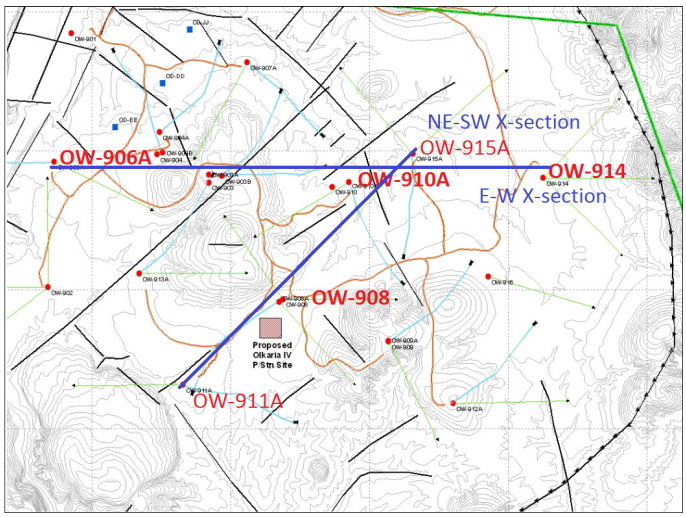

FIGURE 13: Location of geothermal wells and two vertical cross-sections in the Olkaria Domes

zone is in the vicinity of well OW-910A and the coldest around well OW-902. It can be observed from the pressure distribution that the low-pressure zone in well OW-902 coincides well with low temperature. Low-pressure potential indicates areas of rapid heat and mass sink (downflow of fluid and heat loss) while a high potential area indicates zones of fluid and heat inflow/upflow (Grant, 1979). The topography of the terrain also plays a role in pressure distribution. Figure 13 shows the location of wells and two vertical cross-sections. Figures 14 and 15 show the vertical cross-sections of temperature and pressure distributions in W-E and SW-NE directions of the Olkaria Domes field. From the two cross-

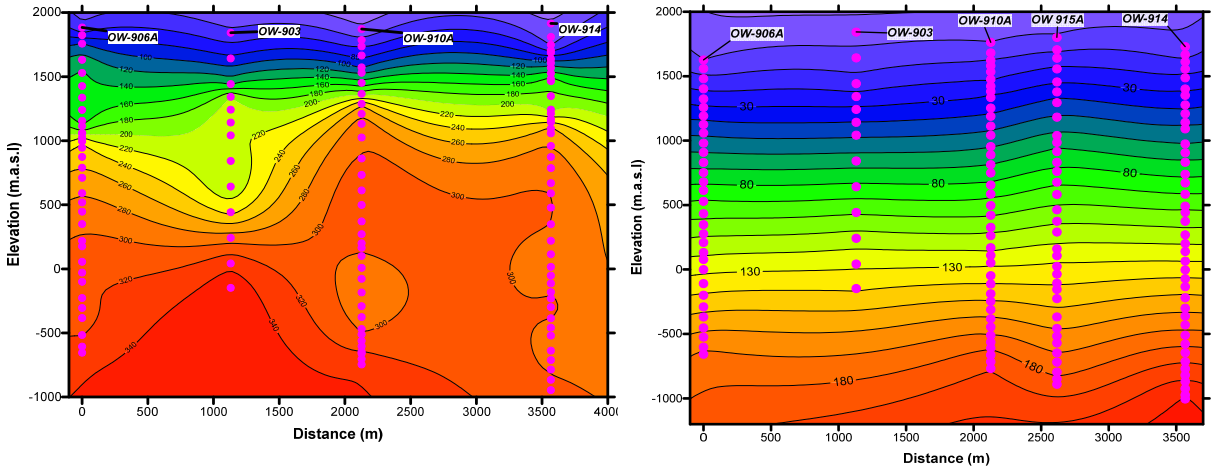

FIGURE 14: W-E cross-sections showing temperature (°C) (left) and pressure (bar-a) (right)

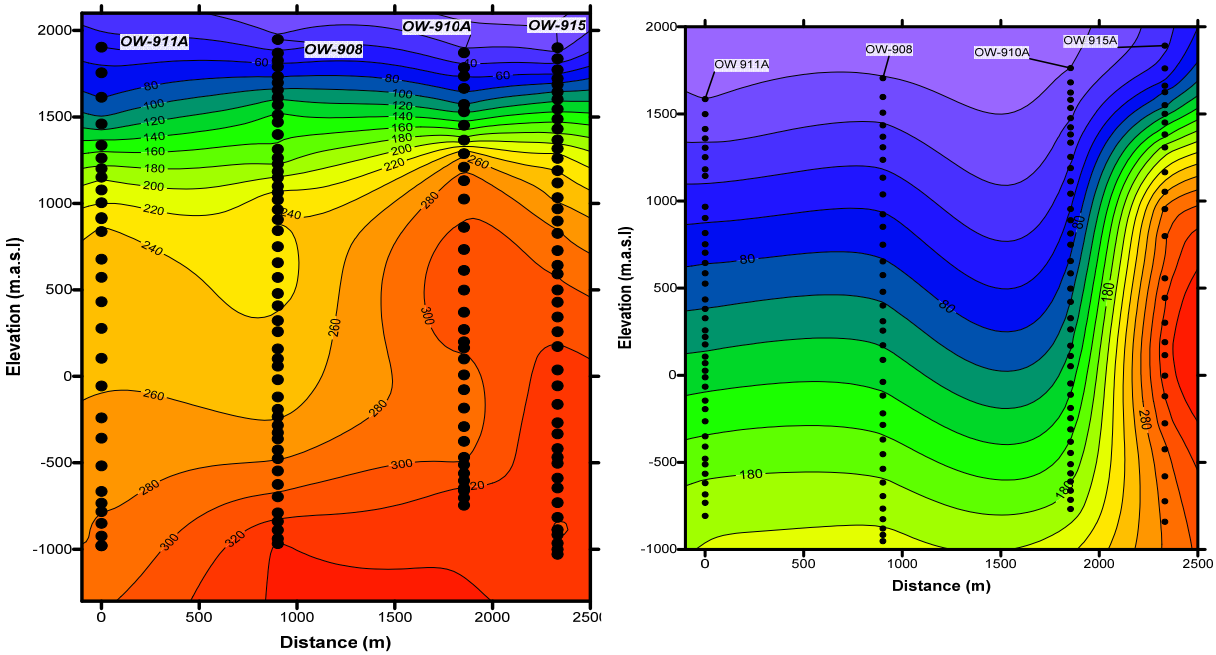

FIGURE 15: SW-NE cross-sections showing temperature (°C) (left) and pressure (bar-a) (right)

sections, the wells seem to have penetrated the hottest part of the reservoir. A hot plume was observed in well OW-903 in the W-E and OW-915 in SW-NE temperature cross-sections, respectively.

3.4 Main results according to the temperature and pressure model

Stable downhole temperature cross-sections across the Olkaria Domes field at 1000, 0 and -600 m a.s.l. (Figures 10, 11 and 12) show peak values in the areas of wells OW-910A, OW-901, OW-903 and OW-909A. Low temperatures were observed in areas around wells OW-902 and OW-902. Well OW-902 happens to have the lowest pressures and there is a possibility of this well being located in the vicinity of a vertical fault zone which may be 230-240°C hot (Odeny, 1999). It is possible that its proximity to the Ol Njorowa gorge could also be a factor.

4. TESTING OF WELLS OW-906A, OW-908, OW-910A AND OW-914

Geothermal well testing and evaluation involves various measurements aimed at gathering information on well characteristics and production potential as well as reservoir properties and conditions. This also includes well simulations with the purpose of enhancing the output of new production wells or existing wells. Well testing plays a key role during exploration drilling, production well drilling, well maintenance and geothermal field monitoring.

The most important properties are the transmissivity and the storativity of the reservoir and permeability of the rock matrix. In Kenya after a successful drilling programme, a typical high-enthalpy well assessment is undertaken through multi-step (usually four steps) injection tests, in order to estimate the main physical properties of the reservoir around the well. Although very valuable information about the undisturbed state of the reservoir can be obtained during drilling, interruptions of the drilling operation to take these measurements are rarely done due to high rig time cost. These measurements should be taken every time there is an interruption in drilling operations, such as when changing the drill bits, as these are the only times available to obtain almost near natural state conditions, especially at the well bottom.

After warm-up a well is discharged to estimate the production potential of the well. Several important flow parameters are monitored during discharge testing: Water and steam flow, temperature or enthalpy of the fluid discharged, non-condensable gas content, dissolved solid content, wellhead pressure, and pressure drop from the reservoir into the well during discharge. During long term testing and utilization, the parameters described above should be measured at regular intervals.

4.1 Injection tests

Injection testing is, in principle, a simple variant of discharge flow testing with the flow reversed. Water is injected into a well and the flow rate is recorded along with changes in down-hole pressure or depth of the water level. A quasi-stable flow versus pressure curve can be obtained, and the transient behaviour measured as changes in flow rate.

Injection is a simple inverse of production if the fluid injected is of the same enthalpy (quality or temperature) as that produced. Generally the fluid injected is water cooler than reservoir temperature and it has different viscosity and compressibility from the reservoir fluid (Grant et al., 1982). The non-isothermal injectivity index obtained from these tests depends on the mobility ratio of the cold region to the hot reservoir and the extent of the cold spot. Storativity, which gives information on the storage and availability of fluid in the reservoir, can be calculated from the data. This is achieved by measuring the pressure at an identified point, preferably the pivot point, which acts as the

representative pressure in the reservoir. If the pressure gauge is not located at the pivot point, and in particular if it is set to a shallower depth, erroneous results are obtained. The oscillatory results obtained are due to the movement of fluids of varying density within the well, causing the pressure differences between the levels to vary with time (Grant et al., 1982). The parameters, i.e. transmissivity, storativity, wellbore storage and skin among others, are evaluated using models based on the pressure diffusion equation.

4.1.1 The pressure differential equation

This equation is used to calculate the pressure (p) in a reservoir at a distance (r) from a production or an injection well producing at a given rate (Q) as a function of time (t). The Theis solution is the most commonly used solution to the differential equation (Earlougher, 1977; Horne, 1995). The following are the assumptions that are used to simplify the situation:

a) The reservoir is homogenous, isotropic, extends to infinity and has a uniform thickness;
b) The flow is considered isothermal and radial;
c) The radius of the wellbore is negligible;
d) The well penetrates the entire formation thickness; and
e) The formation is completely saturated with single-phase fluid.

There are three laws that govern the pressure diffusion equation:

1) *Law of conservation of mass in a given control volume:*

Mass flow in – Mass flow out = Rate of change of mass

$$\rho Q - \left(\rho Q + \frac{\partial(\rho Q)}{\partial r}dr\right) = 2\pi r dr \frac{\partial(\varphi \rho h)}{\partial t}$$

$$-\frac{\partial(\rho Q)}{\partial r} = 2\pi r \frac{\partial(\varphi \rho h)}{\partial t} \tag{2}$$

2) *Law of conservation of momentum, expressed by Darcy's law:*

$$Q = -2\pi r h \frac{k}{\mu}\frac{\partial p}{\partial r} \tag{3}$$

3) *Equation of state of the fluid (fluid compressibility at constant temperature):*

$$c_f = \frac{1}{\rho}\left(\frac{\partial \rho}{\partial p}\right) \tag{4}$$

Combining the three equations above results in the pressure diffusion equation given by:

$$\frac{1}{r}\frac{\partial}{\partial r}\left(\frac{r\partial p(r,t)}{\partial r}\right) = \frac{\mu c_t}{k}\frac{\partial p(r,t)}{\partial t} = \frac{S}{T}\frac{\partial p(r,t)}{\partial r} \tag{5}$$

where $c_t = \varphi c_f + (1-\varphi)c_r$ = Total compressibility;
$c_r = \frac{1}{1-\varphi}\frac{\partial \varphi}{\partial p}$ = Rock compressibility;
$S = c_t h$
$T = kh/\mu$
h = Effective reservoir thickness;
k = Permeability of the rock matrix; and
μ = Dynamic viscosity of the fluid.

The transmissivity *T* is large when fluid and pressure responses travel easily through the reservoir, whereas the storativity *S* describes the storage of the fluid in the reservoir and the amount of the fluid that can be released from the reservoir with a change in pressure.

The radial pressure diffusion equation is a partial differential equation that describes isothermal flow of fluid in a porous medium and how the pressure *P(r,t)* diffuses through the reservoir. Initial and boundary conditions are required to solve for *P(r,t)*. For an infinite acting reservoir, the boundary conditions are:

a) Initial conditions:

$$P\ (r,t) = P_i \quad for\ t = 0, \mathrm{r} > 0 \tag{6}$$

where P_i = Initial reservoir pressure (Pa)

b) Inner and outer boundary conditions:

$$P\ (r,t) = P_i\ r\ \to \infty\ and\ t\ > 0 \tag{7}$$

$$q = 2\pi r \frac{kh}{\mu} \frac{\partial P}{\partial r}\ r \to 0\ and\ t > 0 \tag{8}$$

The solution of the radial pressure diffusion equation, *P(r,t)* , for the above initial time and boundary condition is then:

$$P(r,t) = P_i + \frac{q\mu}{4\pi kh}\ E_i\left(-\frac{\mu c_t r^2}{4kt}\right) \tag{9}$$

E_i is the exponential integral function defined as:

$$E_i(-x) = -\int_x^{\varphi} \left(\frac{e^{-u}}{u}\right) du \quad with \quad x = \left(-\frac{\mu c_t r^2}{4kt}\right) \tag{10}$$

For $x < 0.01 \Rightarrow E_i(-x) = y\ + \ln x,$

where $y\ = 0.5772$ is Euler's constant.

Therefore, if $t\ > \frac{100\mu c_t r^2}{4k}$ and if one uses $\ln x = 2.303 \log x,$ then the solution for the radial pressure diffusion equation can be simplified to:

$$P(r,t) = Pi\ +\ \frac{2.303q\mu}{4\pi kh}\left[log\left(\frac{\mu c_t r^2}{4kt}\right) + \frac{y}{2.303}\right] \tag{11}$$

This solution for the radial pressure diffusion equation is called the Theis solution or the line source solution.

4.1.2 Semi-logarithmic well test analysis

The Theis solution can be written as:

$$P(r,t) - P_i = \frac{2.303q\mu}{4\pi kh}\left[log\left(\frac{4k}{\mu c_t r^2}\right) - \frac{y}{2.303}\right] + \frac{2.303q\mu}{4\pi kh} \tag{12}$$

The above equation is in the form: $\Delta P = A + log\ t$, which is a straight line with slope m on a semilog graph where:

$$\Delta P = P\ (r,t) - P_i;\ A = \frac{2.303q\mu}{4\pi kh}\left[log\left(\frac{4\,k}{\mu c_t r^2}\right) - \frac{y}{2.303}\right],\ \ and\ \ \ m = \frac{2.303q\mu}{4\pi kh} \tag{13}$$

The formation transmissivity, T, can be calculated from the slope of the semi-log straight line by:

$$T = \frac{kh}{\mu} = \frac{2.303\,q\mu}{4\pi kh} \tag{14}$$

If the temperature is known, then the dynamic viscosity μ can be inferred from steam tables, thus, the permeability thickness, kh, may be calculated as follows:

$$kh = \frac{2.303q\mu}{4\pi m} \tag{15}$$

The formation storativity or storage coefficient $\boldsymbol{S = c_t h}$, is then obtained from the intercept with the ΔP axis when the permeability thickness is known. The Theis solution can be written as:

$$\frac{\Delta P}{m} = \left[\left[log\left(\frac{4\,kh}{\mu}\right)\left(\frac{1}{S}\right)\left(\frac{t}{r^2}\right)\right] - \frac{y}{2.303}\right] \tag{16}$$

$$\Longrightarrow 10^{\frac{\Delta P}{m}} = \left(\frac{kh}{\mu}\right)\left(\frac{1}{S}\right)\left(\frac{t}{r^2}\right) \times \left(4 \times 10^{-\frac{\Delta P}{m}}\right) \tag{17}$$

And the storativity can be written as:

$$S = 2.25\left(\frac{kh}{\mu}\right)\left(\frac{t}{r^2}\right) \times 10^{-\frac{\Delta P}{m}} \tag{18}$$

Since the transmissivity $T = {kh}/{\mu}$, then

$$S = 2.2T\left(\frac{t}{r^2}\right) \times 10^{\frac{\Delta P}{m}} \tag{19}$$

Thus, a plot of ΔP vs. log t gives a semi-log straight line response for the infinite acting radial flow period of a well, and is referred to as a *semi-log analysis.* The semi-log analysis is based on the location and interpretation of the semi-log straight line response that represents the infinite acting radial behaviour of the well. However, as the wellbore has a finite volume, it becomes necessary to determine the duration of the wellbore storage effect or the time at which the semi-log straight line begins (Earlougher, 1977; Horne 1995).

4.1.3 Dimensionless variables and type curve well test analysis

Well test analysis often makes use of dimensionless variables in order to simplify reservoir models by embodying the reservoir parameters, thereby generalizing the pressure equations and solutions. They have the advantage of providing model solutions that are independent of any particular unit system. Different reservoir models may have different boundary conditions giving rise to different solutions of the pressure diffusivity equation. Some of the solutions are mathematically complicated and are, therefore, expressed as type curves that are dimensionless solutions associated with a specific reservoir model. Each appropriate reservoir model of a well test is found by plotting pressure transient data

from a well test on a log-log graph and comparing it with various type curves. The following dimensionless variables are substituted in the pressure diffusion equation:

a) Dimensionless pressure, P_D:

$$P_D = \frac{2\pi kh}{q\mu}\left(P_i - P(r,t)\right) \tag{20}$$

b) Dimensionless time, t_D:

$$t_D = \frac{kt}{c_t \mu r^2} \tag{21}$$

c) Dimensionless radius or distance, r_D:

$$r_D = \frac{r}{r_w} \tag{22}$$

Generally, the procedure for type curve analysis can be outlined as follows:

1. The data is plotted as log ΔP vs. log Δt on the same scale as that of the type curve.
2. The curves are then moved, one over the other, by keeping the vertical and horizontal grid lines parallel until the best match is found.
3. The best match is chosen and the pressure and time values are read from fixed points on both graphs: ΔP_m, ΔP_{DM}, Δt_M, and t_{DM}.
4. For an infinite acting system, transmissivity, *T,* is evaluated from:

$$T = \frac{kh}{\mu} = \frac{q}{2\pi}\frac{P_{DM}}{\Delta P_M} \tag{23}$$

5. And the storativity *S* is calculated as:

$$S = c_t h = \frac{kh}{\mu r_w^2}\frac{\Delta t_m}{t_{DM}} \tag{24}$$

4.1.4 Injection testing and analysis

The same injection test procedure was used for all the wells. This involved stationing a temperature/pressure logging tool at an identified depth in a well and then injecting cold water into the well at different pumping rates. The initial flow rate into the well was 0 L/s before pumping began with 16.67 L/s. This lasted for four hours before the pump rate was increased to 21.7, 26 and 31.7 L/s, respectively. The second, third and fourth pumping periods lasted three hours each. The wells under consideration in this report were drilled at different times. The results of the injection testing for wells OW-910A and OW-914 are shown in Figure 16.

A computer program WellTester (Júlíusson et al., 2008), was used in the analysis of the data. A non-linear regression analysis was performed to find the parameters that best fit the data gathered. Many attempts were made using the derivative plot to compare with the trend of different boundary conditions in order to come up with an appropriate model. Only wells OW-914 and OW-910A were used in this analysis due to uncertainties in the data gathered from the other wells. The details on the model selected for the two wells were:

- The reservoir is homogenous;
- Constant pressure boundary; and
- Constant skin and wellbore storage.

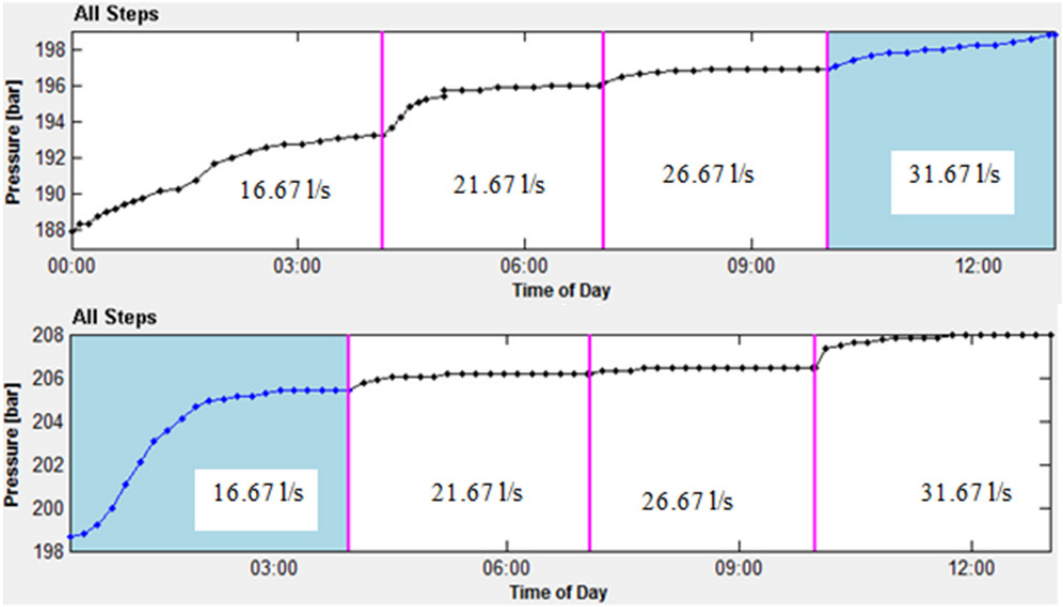

FIGURE 16: The step-pumping steps for wells OW-910A (above) and OW-914 (below)

Only the steps that fit best in the model are presented. Log-linear, log-log scale and the derivative of the pressure response multiplied by the time passed since the beginning for the selected steps are shown for each well. The parameters achieved are the best estimates from the non-linear regression analysis.

OW-914: Only one step fits the model. The plots for the log-log and log-linear scales are shown in Figure 17. The parameters estimated from this one step are given in Table 2.

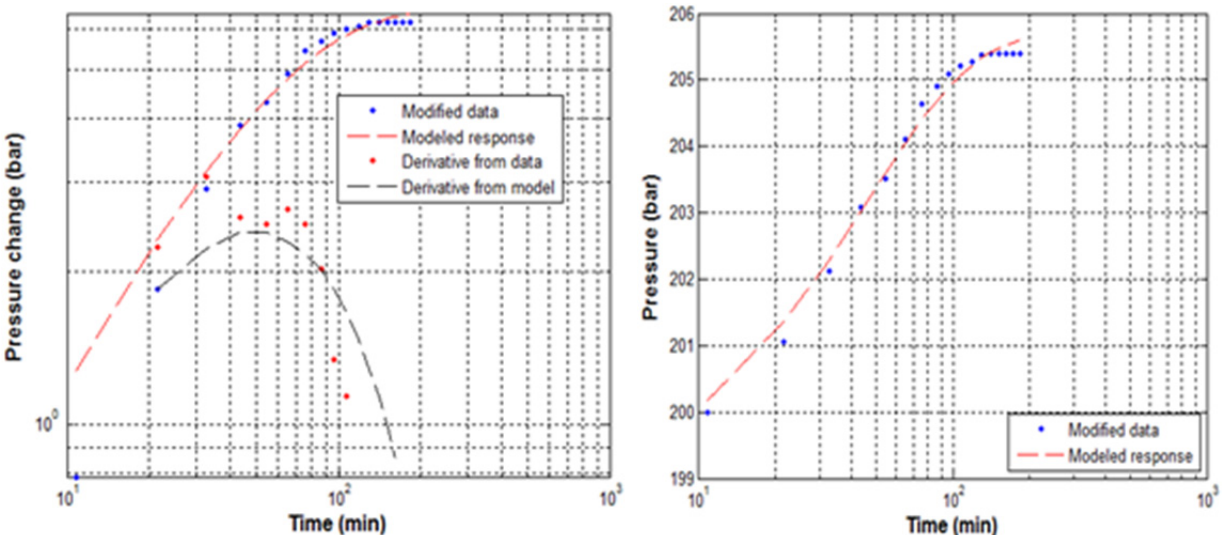

FIGURE 17: OW-914, a fit between model and collected data for step 1 on a log-log scale (left) and on a log-linear scale (right)

TABLE 2: Summary of non-linear regression parameters obtained from injection data in OW-914

Step	Transmissivity (m^3/(Pa s))	Storativity (m^3/(Pa m^2))	Skin factor	Permeability (mD)	Injectivity Index II (L/s)/bar)
Step 1	2.3×10^{-8}	1.5×10^{-8}	- 0.18	4.2	3.55

OW-910A: The pressure tool was stationed at 2600 m depth. Only two steps fit reasonably well to the model and Figures 18 and 19 show the plots from the two steps. The estimated parameters for the two steps are shown in Table 3.

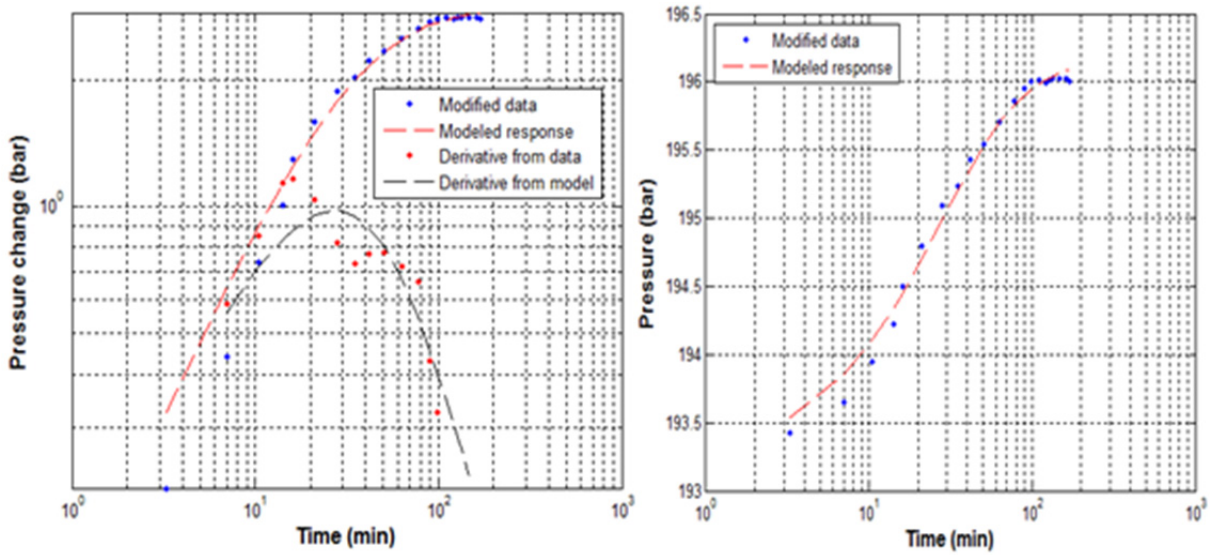

FIGURE 18: OW-910A, a fit between model and collected data for step 2 on a log-log scale (left) and on a log-linear scale (right)

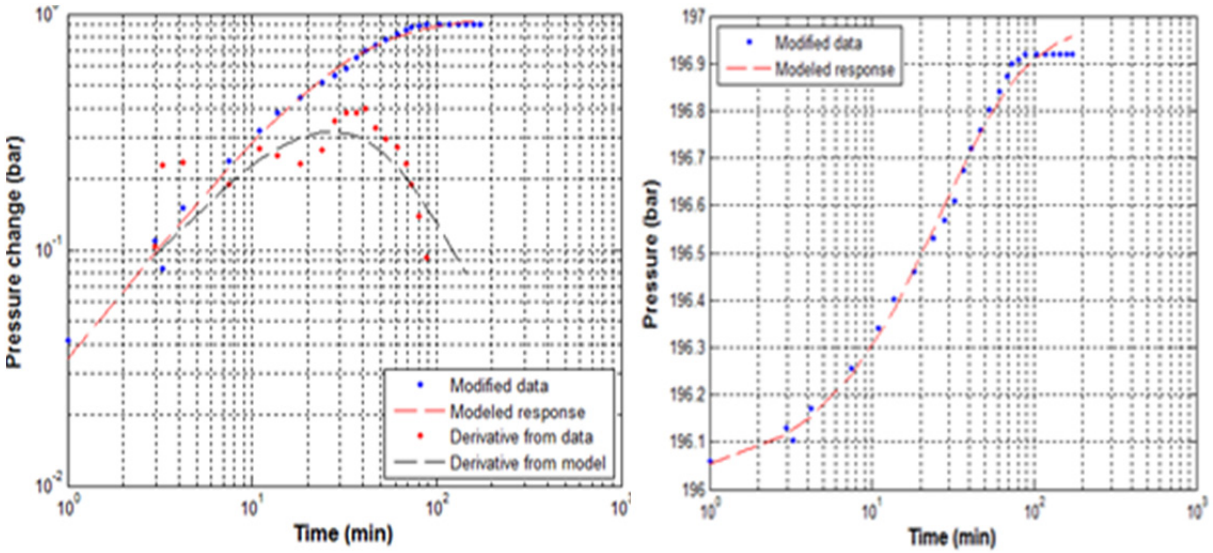

FIGURE 19: OW-910A, a fit between model and collected data for step 3 on a log-log scale (left) and on a log-linear scale (right)

TABLE 3: Summary of non-linear regression parameters obtained from injection data in OW-910A

Step	Transmissivity (m^3/(Pa s))	Storativity (m^3/(Pa m^2))	Skin factor	Permeability (mD)	Injectivity Index II (L/s)/bar)
Step 2	1.5×10^{-8}	2.2×10^{-9}	- 0.4	5.9	3.62
Step 3	4.6×10^{-8}	1.5×10^{-8}	-1.1	3.1	3.62

Working with the data was tedious and many attempts had to be made to get a fit to a certain model. It is suspected that there might be a time and pressure datum shift during data collection. This means

that, at the indicated time, the actual pressure might not have been the one recorded. This is because the pressure transducers take time to stabilize. For this reason, the actual time for the early data might have been different; the error introduced is significant when a logarithmic plot is made. Interpretation of the plot was, therefore, impaired.

The transmissivity values obtained were on the order of 10^{-8} $m^3/(Pa.s)$ and were within the range obtained from the wells directly opposite in the Domes field (Kariuki, 2003). The storativity values were on the order of 10^{-8} $m^3/(Pa.m^2)$, except in OW-910A step one where the storativity value obtained was 2.2×10^{-9} $m^3/(Pa.m^2)$.

The injectivity index (II) was used to estimate the wells' productivity upon completion. The index is useful in deciding the kind of equipment that will be used during discharge tests. The injectivity index values obtained ranged from 3.55 to 3.62 (L/s)/bar.

Permeability is a key factor in the flow potential of a well. It enhances natural convection in the geothermal system. In addition, wells with good permeability have flow paths that connect the wells to reservoir. The permeability values obtained ranged from 3.1 to 5.9 mD.

4.2 Production testing and analysis

Wells in Olkaria Domes are discharge tested after they have been allowed to heat up after drilling for 2-4 months. The well is opened up and allowed to flow to the atmosphere. Geothermal high-temperature wells are usually discharged into a silencer which also acts as a steam-water separator at atmospheric pressure. The two-phase mixture is made to flow through different sizes of lip pressure pipes into the silencer. The steam disappears into the atmosphere but the liquid water is measured as it flows from the silencer over a V-notch weir. The following flow parameters are then measured:

- Wellhead pressure (WHP);
- Lip pressure (Pc);
- Height of water in the V-notch weir.

Using the Russel James lip pressure method (Equation 25), the output parameters from the discharging well are calculated (Grant et al., 1982):

$$Q = 1{,}835{,}000\, A\, \frac{P_c^{0.96}}{H^{1.102}} \tag{25}$$

where Q = Total mass flow rate (kg/s)
A = Cross-sectional area of the lip pipe (m^2)
Pc = Critical pressure at the end of the lip pipe (bar-a)
H = Fluid enthalpy (kJ/kg).

Since the well is being discharged into the atmosphere, the specific enthalpies of steam and water at atmospheric pressure should be used:

$$Q = W\frac{(Hs - Hw)}{(Hs - H)} \tag{26}$$

$$Q = W\frac{2256}{(2676 - H)} \tag{27}$$

where W = Water fluid flow (kg/s);
Hs = Steam enthalpy at atmospheric pressure (kJ/kg);
Hw = Water enthalpy at atmospheric pressure (kJ/kg).

Combining Equations 25 and 27, gives:

$$1{,}835{,}000A\frac{P_c^{0.96}}{H^{1.102}} = W\frac{2256}{(2676-H)} \tag{28}$$

The enthalpy H is the only unknown variable in Equation 28 and, after obtaining it from Equation 27, the following parameters were calculated:

- Total mass flow rate;
- Water flow rate;
- Steam flow rate;
- Flow enthalpy;
- Electrical power.

A well discharging on a 8'' lip pipe should give the maximum flow and the lowest enthalpy. Throttling of the well by use of a smaller diameter lip pipe is expected to result in a lower mass flow rate at a higher WHP.

4.2.1 Analysis of discharge data

OW-914: Initial self-sustaining discharge was possible due to the presence of wellhead pressure; discharge was started by simply opening the wellhead control valve (Figure 20). This well was tested with four lip pressure pipes (4, 5, 6 and 8"). It was not tested on the 3" lip pipe. The reason was to allow the rig to come back to the same well pad to drill OW-914A. Table 4 shows an average output summary for this well.

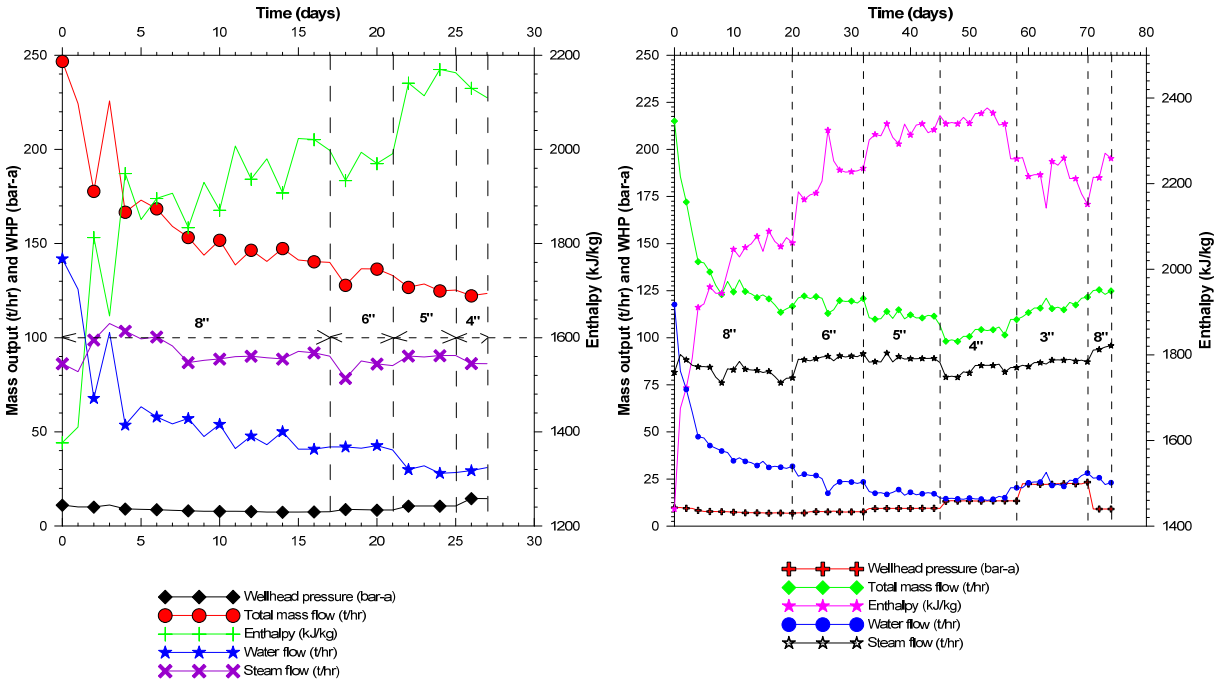

FIGURE 20: Discharge history of OW-914 (left) and OW-910A (right)

TABLE 4: OW-914 discharge output summary

Lip pipe size (")	WHP (bar-a)	Mass flow (t/hr)	Steam flow (t/hr)	Enthalpy (kJ/kg)
8	6.54	155.87	92.8	1908.7
6	8.63	150.60	84.3	1972.8
5	10.2	140.02	90.3	2146.8
4	12.2	118.9	86.3	2120.0

OW-910A: This well is a big producer with 13 MWe. The well could initiate self-discharge and therefore there was no need for air lifting (Figure 20). It showed a high mass flow rate (215.1 t/hr) for the first few hours after starting the discharge, which was later reduced. This was assumed to be a wellbore storage effect. For almost constant wellhead pressure, enthalpy and flow rate cycles were achieved for most of the test period but with higher averages and weighted averages (Table 5).

TABLE 5: OW-910A discharge output summary

Lip pipe size(")	WHP (bar-a)	Mass flow (t/hr)	Steam flow (t/hr)	Enthalpy (kJ/kg)
8	7.8	165.69	82.60	1920.6
6	9.17	159.75	90.7	2224.0
5	10.85	148.21	88.6	2323.3
4	13.4	123.05	83.0	2336.3

TABLE 6: OW-908 discharge output summary

Lip pipe size (")	WHP (bar-a)	Mass flow (t/hr)	Steam flow (t/hr)	Enthalpy (kJ/kg)
8	4.33	59.90	25.2	1672.4
6	5.68	53.94	22.0	1964.3
5	7.41	46.25	22.6	2062.0
4	9.67	35.76	17.9	2104.1
3	10.98	27.34	23.9	2251.2

OW-908: This well has a capacity of 4 MWe. It was discharged for about three months. The prevailing conditions after three months showed that the WHP was less than 5 bar-a on 8" lip pipe (Figure 21). An average of the output data per lip pipe was computed and is shown in Table 6. The values of the flow rate are averages while those of enthalpy are weighted averages.

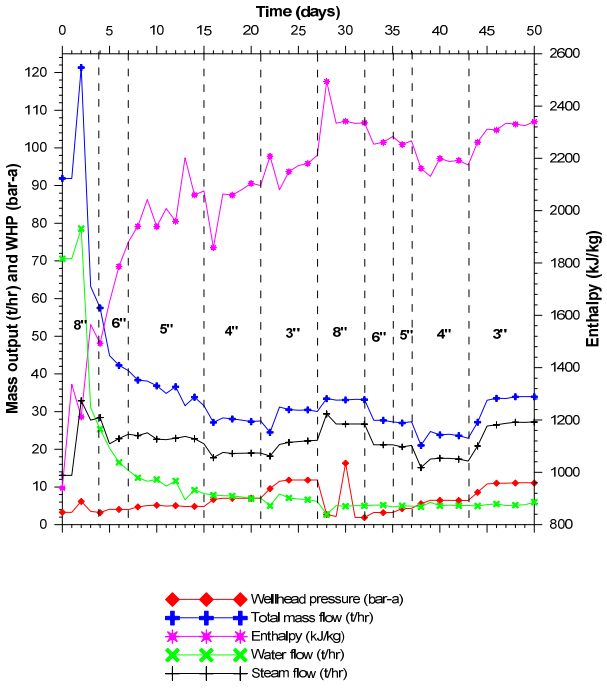

FIGURE 21: Discharge history of OW-908

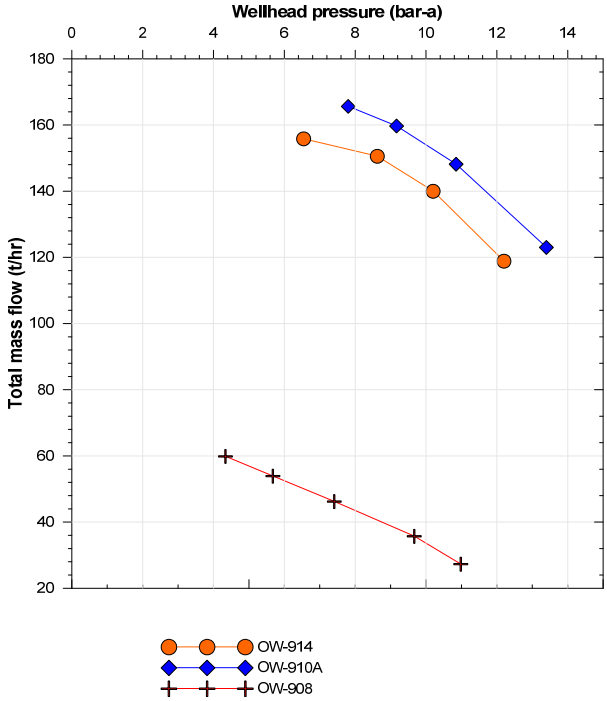

FIGURE 22: The output curves for the Domes wells

4.2.2 Wellhead output curves

The wellhead output or characteristic curve is used to relate the total mass flow rate of a well to its wellhead pressure. The total mass flow rate results obtained from the output tests at different throttle conditions should form a smooth curve when plotted against wellhead pressure. Well OW-906A could not sustain discharge and, therefore, was not included in this plot (Figure 22). From Figure 22, it can be observed that well OW-910A gave the highest mass flow at all wellhead pressures. Well OW-914 showed more stable values with a maximum discharge pressure (MDP) of about 12.2 bar-a.

5. CONCEPTUAL MODEL OF OLKARIA DOMES FIELD

Modelling of a geothermal system is done to help obtain information and to understand the conditions in a reservoir as well as the nature and properties of the system. Depending on the amount of data available, the model can be used to predict the response of the reservoir to future production and to estimate the production potential of the system. The outcome of different management actions can be predicted (Grant et at., 1982). The most appropriate modelling approach is determined by the availability of data, time, cost and the objective of a particular study. Very limited time was available for this study, therefore, only a preliminary conceptual model was developed.

In order to define a conceptual reservoir model of Olkaria Domes field, several temperature and pressure plane-sections for the whole area and profiles for the different wells were plotted. Analysis of the plots shows that the wells to the west of Domes have low pressures (Figure 10). Recharge to the Olkaria Domes is to the north around OW-905A and could be attributed to the NW-SE trending Gorge Farm fault (Figure 3). Bottomhole temperature and pressure for well OW-903 showed an inflow of cooler fluid at 1000 m depth which distorts the temperature and pressure contours (Kariuki, 2003). Analysis of nitrogen gas concentrations in the Olkaria wells showed maximum values in the Domes field around OW-903, indicating inflow of shallow, atmospherically contaminated water into the well (Karingithi, 2002). The water inflow could be due to the NNE-SSW trending fault (Figure 3) which seems to have been intercepted by well OW-903 at 1000 m depth. From Figures 11, 12, 14, 15 and 23, the likely upflow zone for the Olkaria Domes is located in the eastern part of the field towards the ring structure of the field around wells OW-909, OW-910, OW-914 and OW-915. These wells showed boiling point with depth profiles which were taken here as indicators of an upflow zone in their vicinity. Well OW-902 seems to have been drilled in an outflow zone (Kariuki, 2003) and this explains why the pressure decreases towards the western part of the Domes Field.

Wells within the vicinity of the upflow zone, e.g. 910A, 914, 915A and 916, registered higher mass outputs and maintained the flow even at higher wellhead pressures (Figure 24). Wells in the eastern part of Domes have higher enthalpies (range between 2250 and 2500 kJ/kg), whereas the wells in the western part have low enthalpies, with well OW-902 having the lowest one at 1100 kJ/kg.

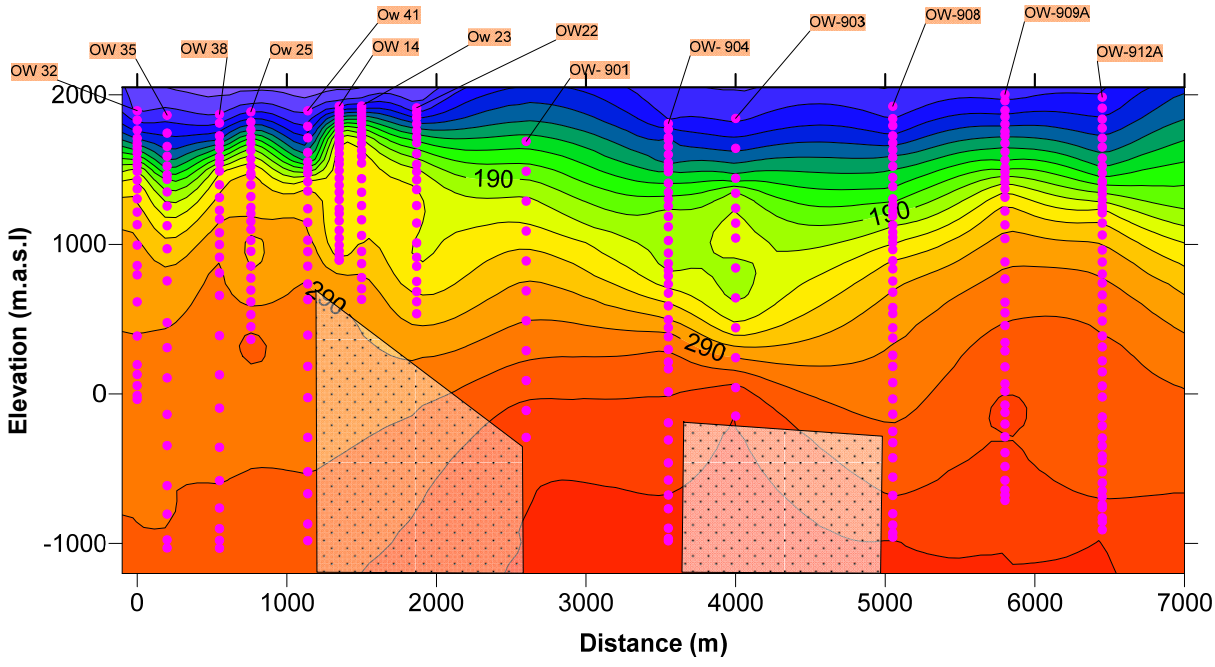

FIGURE 23: NW-SE temperature cross-section connecting Olkaria Domes to Olkaria Northeast

5.1 Volumetric resource assessment

Reserve estimation is one of the main tasks of reservoir evaluation. Any development cannot continue without the assurance that the field has the reserve capacity to produce over the desired life of the field. In this project, volumetric calculations were carried out using the Monte Carlo simulation method. This method is used to deal with complex scenarios that describe the distribution of known reservoir parameters by using uncertainty or probability distribution (Halldórsdóttir et al., 2010). For the simplicity of analysis here, some parameters were assumed to have either triangular or uniform distribution while others were given fixed values. Table 7 shows the parameters used for the analysis of the power output for a 30 year production period for the Olkaria Domes geothermal field.

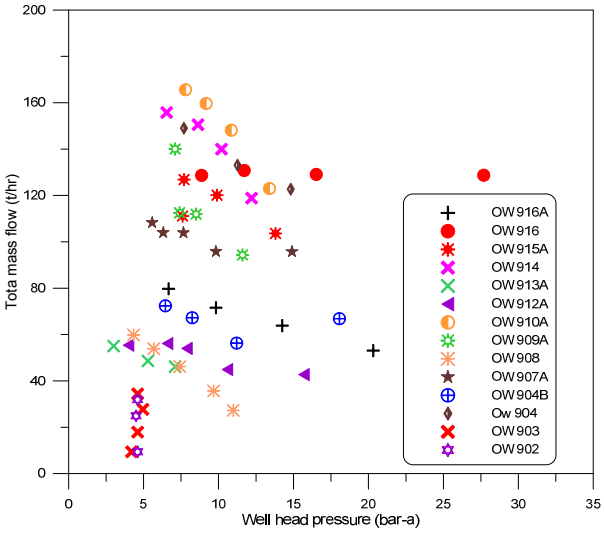

FIGURE 24: Output characteristics curve for Domes wells

TABLE 7: Parameters used in Monte Carlo analysis for Olkaria Domes geothermal field

Parameter	Minimum value	Best value	Maximum value	Distribution Type
Area (km^2)	23	27	36	triangular
Upper depth (m)		0		Fixed
Lower depth (m)		3000		Fixed
Temperature at upper depth (°C)		30		Fixed
Cut-off temperature (°C)		170		fixed
Porosity (%)	8		10	uniform
Specific heat of rock (J/kg °C)	900		980	uniform
Density of rock (kg/m^3)		2900		fixed
Specific heat of water (J/kg °C)		5200		fixed
Density of water (kg/m^3)	700		800	uniform
Boiling curve ratio (%)	80	90	100	triangular
Recovery factor (%)	10	20	25	triangular
Convergence efficiency (%)		12		fixed

According to the probability distribution in Figure 25, it is most probable (7% probability) that the electrical power production capacity lies between 485 and 505 MWe if the recoverable heat is used for 30 years. It can also be seen that the volumetric model predicts with 90% confidence that the power production capacity lies between 340 and 760 MWe for a 30 year production period. From cumulative probability distribution in Figure 25, it can be seen that the volumetric model predicts with 90% probability that at least 380 MWe could be produced from Olkaria Domes field for a production period of 30 years.

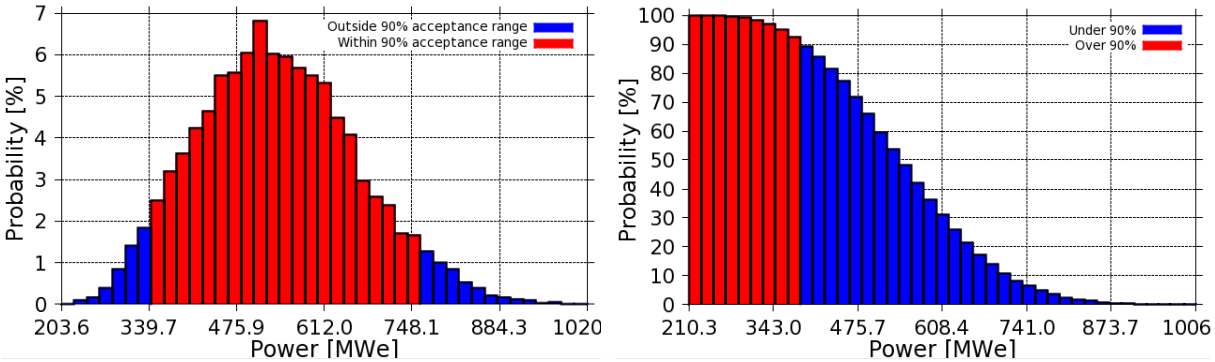

FIGURE 25: Simple probability distribution (left) and cumulative distribution (right) for electric power generation

6. SIMPLE NUMERICAL MODEL OF OLKARIA DOMES

The first 3-dimensional natural state model for the Greater Olkaria geothermal area was developed in 1987 by Bodvarsson and Pruess (1987). A simple numerical model for the Olkaria Domes field was developed for this project. The model covers an area of about 27 km^2 and was partitioned into 31 grid blocks (Figure 26). The natural state simulation run was done for 10,000 years using the TOUGH2 numerical simulator (Pruess et al., 1999) until a steady-state situation agreed closely with the measured temperature values in most parts of the field.

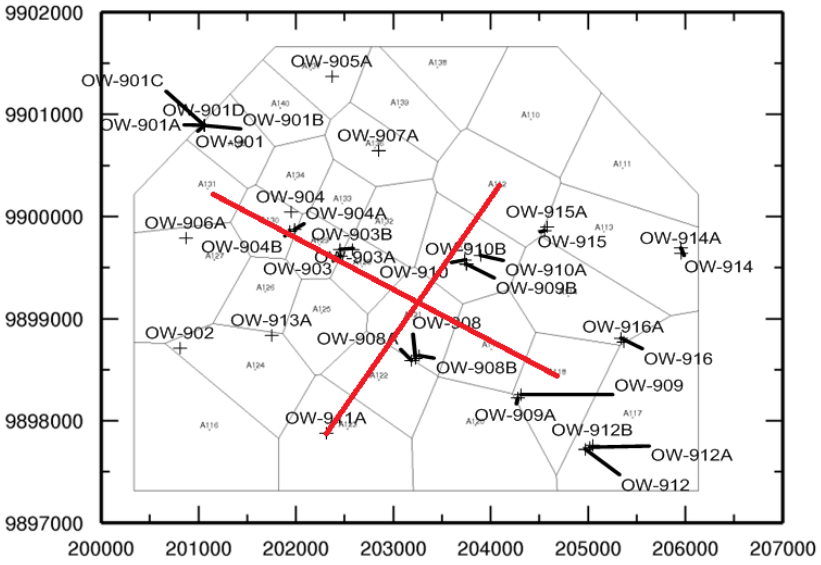

FIGURE 26: The horizontal numerical grid; reservoir fluids were assumed to be pure water and all properties were based on steam tables. A rock type with defined rock properties (values of permeability, porosity, density and thermal conductivity) was assigned to each model element

Vertically, the model assumes an impermeable cap rock with a thickness of 700 m beneath which is a permeable reservoir of 2300 m (Figure 27) that is further partitioned into nine layers giving a total of 279 grid blocks. The temperature and pressure in the top and bottom layers of the model were set constant as boundary conditions and made inactive during the simulation run.

The hot upflows were implemented as sources of heat and fluid at layer H of the model. It was a long trial and error procedure, slightly changing the rock parameters and boundary conditions, to fit the modelled values with selected data. Important adjustable parameters in the model were the strength of the upflow (both enthalpy and upflow rate) as shown in Table 8, and vertical and horizontal permeabilities along the prominent hydrogeologic structures. The model's calculated formation temperature values were compared with the estimated formation temperature. The formation temperature was also estimated using the Berghiti method and is shown as red dots (Figures 28).

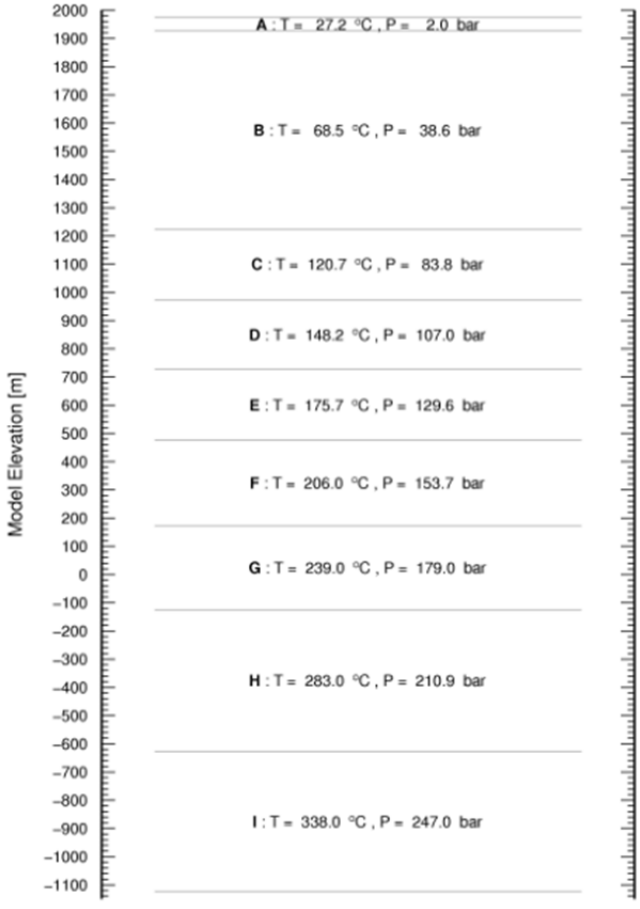

FIGURE 27: The vertical numerical grid

TABLE 8: Upflow rates and enthalpies

Upflow area	Flow rate (kg/s)	Enthalpy (kJ/kg)
HA114SOU01	9	1600
HA115SOU01	8.5	1600
HA119SOU01	7	1600
AA116HVE01	3×10^{-10}	5.0×10^{5}
AA127HVE01	3×10^{-10}	5.0×10^{5}

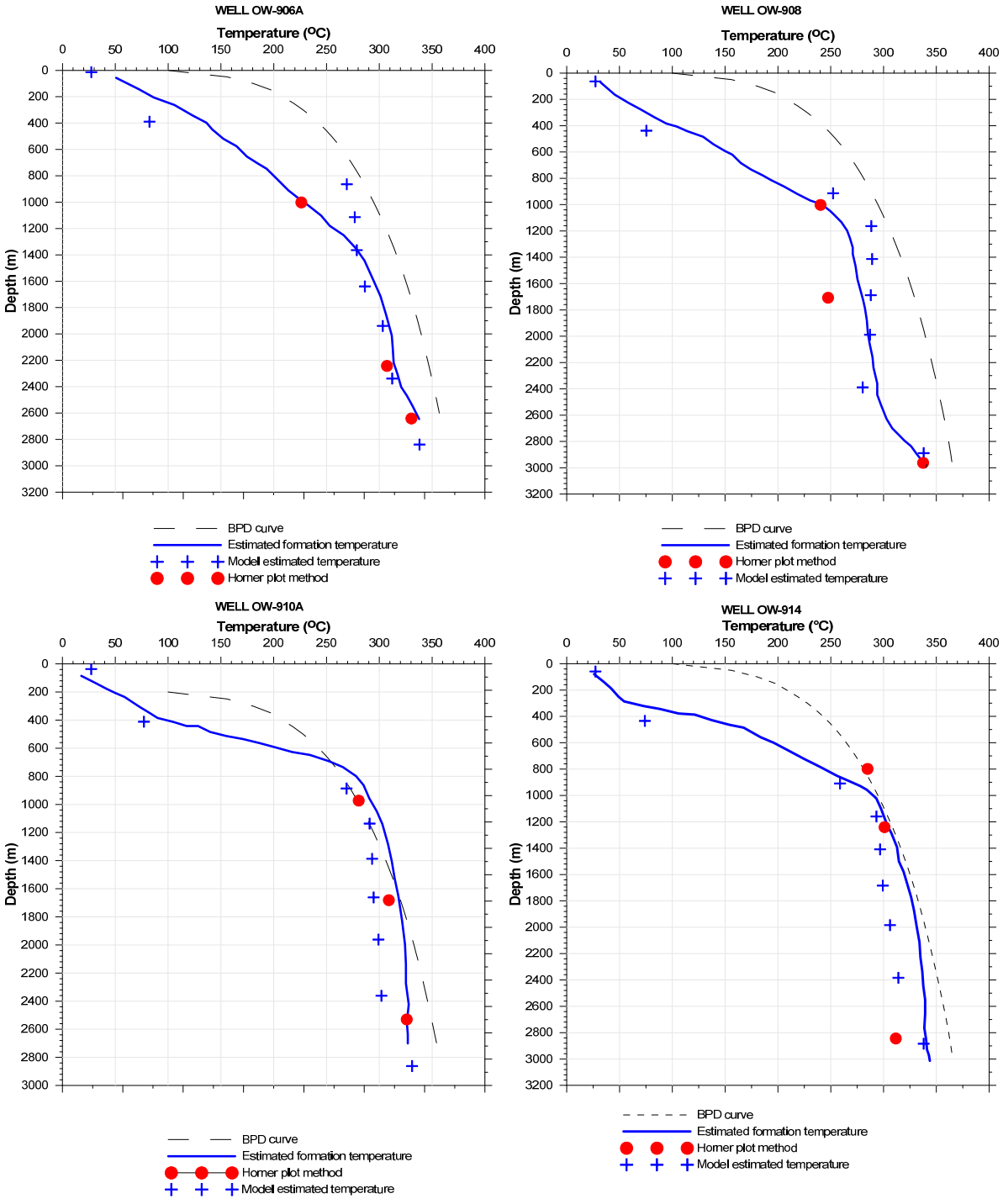

FIGURE 28: Comparison between modelled and estimated formation temperatures

7. DISCUSSION AND CONCLUSIONS

Olkaria Domes geothermal field can be classified as a high-temperature and high-enthalpy field. The field is in a two-phase condition with the temperature and pressure following the boiling point with depth curve; logging revealed temperatures of over 300°C in most of the wells at a depth of about 2000 m. Wells OW-910A and OW-914 showed a boiling with depth curve (BPD) profile, suggesting that they were drilled in or near an upflow zone. The upflow zone of the Olkaria Domes field is likely to be located in the eastern part of the field.

The recharge to the Olkaria Domes geothermal field is from the north. The fluid flow appears to be generally from the north to the southwest. Well OW-902 seems to have been drilled in an outflow zone which coincides well with low pressures and temperatures, indicating an area of rapid heat and mass sink. There is an intrusion of cooler fluids in well OW-903 at a depth of about 1000 m. The well seems to have intercepted a fault bringing in cold water (Kariuki, 2003). Analysis of nitrogen gas concentrations in Olkaria Domes wells shows maximum values in this well, indicating inflow of shallow atmospherically contaminated water into well OW-903 (Karingithi, 2002).

The volumetric analysis estimate shows that Olkaria Domes geothermal field can support at least 380 MWe for about 30 years with 90% confidence. Well test analysis indicate transmissivities ranging from 1.5 to 4.6 $\times$ 10^{-8} m^3/Pa.s and effective permeabilities in the range 3.1-5.9 mD in the reservoir, with negative skin being observed in most of the wells.

ACKNOWLEDGEMENTS

I would like to express my gratitude to Dr. Ingvar B. Fridleifsson and Mr. Lúdvík S. Georgsson for the chance to study, and I greatly appreciate the support from the UNU-GTP programme. I appreciate Ms. Thórhildur Ísberg, Mr. Markús A.G. Wilde and Mr. Ingimar G. Haraldsson for their great assistance during my study and stay in Iceland. Sincere thanks to my supervisors, Ms. Saeunn Halldórsdóttir, Ms. Sigrídur Sif Gylfadóttir and Dr. Andri Arnaldsson for their tireless assistance and advice during my research project. To you I say, many thanks for imparting very valuable knowledge to me. I´m grateful to my employer, Kenya Electricity Generating Company Ltd (KenGen), for granting me sabbatical study leave and providing data for use in this project. Thanks to Mr. Felix Mwarania, among other KenGen staff, who worked tirelessly to ensure I got all the required data. I also would like to give my appreciation for the knowledge shared with my colleague, Mr. Vincent Kipkirui Koech throughout my project.

Last, and definitely not least, I am very grateful to my wife, Carolyne Mutheu, and to our daughter Bridgit Ndanu. I owe you two everything. You endured my long absence. It would have been impossible for me to go through this training without your support, prayers, and encouragement. Thanks a million times and God bless you. I'm grateful to God for his grace and protection throughout my stay in Iceland and for keeping my beloved family safe.

REFERENCES

Arason, Th., and Björnsson, G., 1994: *ICEBOX* (2nd edition). Orkustofnun, Reykjavík, 38 pp.

Arason, Th., Björnsson, G., Axelsson, G., Bjarnason, J.O., and Helgason, P., 2003: *The geothermal reservoir engineering software package Icebox, user´s manual.* Orkustofnun, Reykjavik, man., 53 pp.

Björnsson, G., 2011: *Two-phase flow in reservoirs and wells.* UNU-GTP, Iceland, unpublished lecture notes.

Bodvarsson, G.S., and Pruess, K., 1987: *Numerical simulation studies of the Olkaria geothermal field.* Kenya Power Company Ltd., internal report.

Earlougher, R.C., 1977: *Advances in well test analysis.* Soc. Petr. Eng., Monograph 5, 264 pp.

Giggenbach, W.F., 1991: Chemical techniques in geothermal exploration. In: D'Amore, F. (coordinator), *Application of geochemistry in geothermal reservoir development*. UNITAR/UNDP publication, Rome, 119-142.

Grant, M.A., 1979: *Interpretation of downhole measurements in geothermal wells.* DSIR, Wellington, New Zealand, report 8, AMD-88, 66 pp.

Grant, M.A., Donaldson, I.G., and Bixley, P.F., 1982: *Geothermal reservoir engineering.* Academic Press, NY, 369 pp.

Halldórsdóttir, S., Björnsson, H., Mortensen, A.K., Axelsson, G., and Gudmundsson, Á., 2010: Temperature model and volumetric assessment of the Krafla geothermal field in N-Iceland. *Proceedings, World Geothermal Congress 2010, Bali, Indonesia*, 10 pp.

Helgason, P., 1993: *Step by step guide to BERGHITI. User´s guide.* Orkustofnun, Reykjavik, 17 pp.

Horne, R.N., 1995: *Modern well test analysis, a computer aided approach (*2nd edition). Petroway Inc., USA, 257 pp.

Júlíusson, E., Grétarsson, G., and Jónsson, P., 2008: *WellTester.1.0b. User´s guide.* ISOR – Iceland GeoSurvey, Reykjavík, report 2008/63, 26 pp.

Karingithi, C.W., 2002: *Hydrothermal mineral buffers controlling reactive gas concentrations in the Greater Olkaria geothermal system, Kenya.* University of Iceland, MSc thesis, UNU-GTP, Iceland, report 2, 51 pp.

Kariuki, M.N., 2003: Reservoir assessment and wellbore simulations for the Olkaria Domes geothermal field, Kenya. Report 14 in: *Geothermal training in Iceland 2003*. UNU-GTP, Iceland, 337-360.

Lagat, J.K., 1995: Borehole geology and hydrothermal alteration of well OW-30, Olkaria geothermal field, Kenya. Report 6 in: *Geothermal training in Iceland 1995*. UNU-GTP, Iceland, 135-154.

Lagat, J.K., 2004: *Geology, hydrothermal alteration and fluid inclusion studies of the Olkaria Domes geothermal field, Kenya.* University of Iceland, MSc thesis, UNU-GTP, Iceland, report 1, 79 pp.

Malimo, S.J., 2009: Interpretation of geochemical well test data for wells OW-903b, OW-904b and OW-909, Olkaria Domes, Kenya. Report 17 in: *Geothermal training in Iceland 2009*. UNU-GTP, Iceland, 319-344.

Mariita, N.O., 2010: Exploration history of Olkaria geothermal field by use of geophysics. *Presentation at "Short Course V on Exploration for Geothermal Resources, UNU-GTP, KenGen, and GDC, Lake Bogoria and Lake Naivasha, Kenya,* 13 pp.

Odeny, O.N.J., 1999: Analysis of the downhole data and preliminary production capacity estimate for the Olkaria Domes geothermal field, Kenya. Report 11 in: *Geothermal training in Iceland 1999*. UNU-GTP, Iceland, 285-306.

Omenda, P.A., 1998: The geology and structural controls of the Olkaria geothermal system, Kenya. *Geothermics, 27-1*, 55-74.

Pruess, K., Oldenburg, C., and Moridis, G., 1999: *TOUGH2 user´s guide, version 2.* Lawrence Berkeley National Laboratory, University of California, Berkeley, Ca.

Were, J.O., 2007: *The speciation of trace elements in spent geothermal fluids and implications for environmental health around Olkaria, Kenya*. University of Iceland, MSc thesis, UNU-GTP, Iceland, report 1, 73 pp.